

**Gene Co-expression Network Analysis to Identify Key Genes involved in the  
Development of Root-knot nematode *Meloidogyne incognita***

**MOSIOMA NEHEMIAH ONGESO**

**I56/11793/2018**

**A thesis submitted in partial fulfillment for the degree of Master of Science in  
Bioinformatics in the University of Nairobi**

**©April 2023**

## Declaration

This thesis is my original work and has not been presented for a degree in any other University.

Signature: *nongeso*

Date: **26th April 2023**

MOSIOMA NEHEMIAH ONGESO

I56/11793/2018

## Supervisors' Approval

This thesis has been submitted for examination with our approval as university supervisors.

Dr. Rosaline Wanjiru Macharia, PhD

Department of Biochemistry,

University of Nairobi.

Signature: ..... *Macharia RW* ..... Date: ..... 26th April, 2023 .....

Dr. Solveig Haukeland, PhD

Plant Health Theme,

International Centre of Insect Physiology and Ecology.

Signature: ..... *Su* ..... Date: ..... 30th April 2023 .....

## **Dedication**

Every adventure necessitates self-effort and the guidance of seniors, particularly those who are near to our hearts. My humble attempt is dedicated to my dear and loving Father and Mother, who showered me with care, love, encouragement, and daily prayers—not forgetting my dedicated and well-respected mentors.

## Acknowledgement

I thank God for providence, health, lessons learned, friends made, collaborations, and challenges throughout the study period. Scientific research and learning are not a one-man show; that's why I would like to thank those who significantly contributed to this thesis. First and foremost, I would like to express my gratitude to Dr. Rosaline Macharia. She was a tremendous mentor, guide, and supervisor who allowed me to grow as a scientist during my research. I am also grateful to thank Dr. Solveig Haukeland and the NemAfrica Laboratory for hosting me and providing feedback on my work.

I greatly acknowledge the University of Nairobi and the Department of Biochemistry for creating a favorable environment to further my studies. My further appreciation goes to The Pan African Network for Bioinformatics Training (H3ABioNet) through Caleb Kibet and Andrew Espira of the International Centre of Insect Physiology and Ecology (*icipe*) node for providing the necessary computational infrastructure and invaluable support to bring this thesis to a good end. Special gratitude to the Centre for Agriculture and Bioscience International (CABI) for financially supporting my research.

Special thanks to Kennedy Mwangi and John Gitau for their assistance in troubleshooting the analysis scripts. I am grateful for the contributions of Prof Danny Coyne, Felix Matheri, Stephen Okeyo, and Winfred Gatua for your valuable input and support during this project. I recognize Grace Nyambura, Newton Nyagah, and Agnes Kiriga for your assistance in understanding, extracting, and classifying plant-parasitic

nematodes, and much grace to Mr. Elias Mwangi for language editing and formatting of the thesis.

I am grateful to my parents, Richard Mosioma and Grace Kwamboka, for all the prayers and sacrifices to sustain me this far. To my beloved Delphine Moraa, I am humbled by your morale support and unfailing love. I convey my hearty appreciation to my siblings, Joshua Okong'o, Deborah Nyangige, and Keziah Mokeira, for their unaverted support. Further, I extend my gratitude to Timoteo Ombati, and Mr. and Mrs. Washington Opiyo for their calls to check up on me and raise my hopes.

Finally, I am encouraged and privileged by all who directly and indirectly influenced my study, and I wish them all God's blessings.

## Table of Contents

<b>Declaration.....</b>	<b>ii</b>
<b>Dedication .....</b>	<b>iii</b>
<b>Acknowledgement .....</b>	<b>iv</b>
<b>Table of Content.....</b>	<b>vi</b>
<b>List of Figures.....</b>	<b>ix</b>
<b>List of Table.....</b>	<b>x</b>
<b>List of Appendices.....</b>	<b>xi</b>
<b>List of Abbreviations .....</b>	<b>xiii</b>
<b>ABSTRACT.....</b>	<b>xiv</b>
<b>CHAPTER ONE .....</b>	<b>1</b>
<b>1.0 INTRODUCTION.....</b>	<b>1</b>
1.1 Background Information.....	1
1.2 Statement of the Problem .....	3
1.3 Research Question .....	5
1.4 Study Objectives.....	5
1.5 General Objective .....	5
1.6 Specific Objectives .....	5
1.7 Justification of the Study .....	6
<b>CHAPTER TWO .....</b>	<b>7</b>
<b>2.0 LITERATURE REVIEW .....</b>	<b>7</b>
2.1 Nematodes .....	7
2.2 Nematodes of Economic Significance.....	8
2.3 Taxonomy of Plant Parasitic Nematodes.....	9
2.4 The <i>Meloidogyne</i> genus .....	10
2.5 The lifecycle of <i>Meloidogyne</i> species .....	11
2.6 Diagnosis and prevention of <i>Meloidogyne incognita</i> Infestation .....	14
2.7 Plant-Nematode Interaction.....	17
2.8 Cellular immune response in plants.....	25
2.9 Co-expression Networks.....	27
2.10 Functional Enrichment of Module Genes.....	32
2.11 Regulatory Motif Finding.....	34

<b>CHAPTER THREE</b> .....	<b>37</b>
<b>3.0 MATERIALS AND METHODS</b> .....	<b>37</b>
3.1 Data Acquisition .....	37
3.2 Data Pre-processing .....	37
3.3 Generation of gene-co-regulation matrix .....	37
3.4 Pre-processing of the gene co-expression Matrix.....	38
3.5 Gene co-expression network construction.....	39
3.6 Function Enrichment Analysis .....	40
3.7 Regulatory Motif Finding.....	40
<b>CHAPTER FOUR</b> .....	<b>42</b>
<b>4.0 RESULTS</b> .....	<b>42</b>
4.1 A weighted gene co-expression network of <i>Meloidogyne incognita</i> .....	42
4.2 Scale-free topology for Adjacency Matrix Construction .....	43
4.3 Detection of Modules and hub genes in the gene co-expression network of <i>M. incognita</i> .....	45
4.4 Functional enrichment of identified Modules and hub genes in the gene-co-expression network of <i>M. incognita</i> .....	50
4.5 Gene set enrichment to determine module molecular function.....	50
4.6 Gene set enrichment of hub genes. ....	51
4.7 Identification of 3' untranslated regions (UTR) based on gene co-expression modules.....	52
<b>CHAPTER FIVE</b> .....	<b>55</b>
<b>5.0 DISCUSSION</b> .....	<b>55</b>
5.1 Construction of a weighted gene co-expression network of <i>Meloidogyne incognita</i> .....	55
5.2 Functional enrichment of identified Modules and hub genes in the gene-co- expression network of <i>M. incognita</i> .....	56
5.3 Identification of 3' untranslated regions (UTR) based on gene co-expression modules.....	60
<b>CHAPTER SIX</b> .....	<b>62</b>
<b>6.0 CONCLUSIONS, LIMITATIONS AND RECOMMENDATIONS</b> .....	<b>62</b>
6.1 Conclusions .....	62
6.2 Limitations.....	62
6.3 Recommendations .....	62

<b>REFERENCES.....</b>	<b>64</b>
<b>Appendices.....</b>	<b>91</b>



## List of Figures

<b>Figure 2.1:</b> The five developmental stages of genus <i>Meloidogyne</i> .....	14
<b>Figure 4.1:</b> A hierarchical clustered heat map showing correlation of <i>M. incognita</i> gene expression between different developmental stages.....	42
<b>Figure 4.2:</b> Illustration of scale free topology of determining adjacency matrix function for constructing <i>M. incognita's</i> gene co-expression network. ....	44
<b>Figure 4.3:</b> An illustration of modules in the gene-gene co-expression network of <i>M. incognita</i> .....	45
<b>Figure 4.4(a):</b> An illustration of the gene co-expression networks and modules of <i>M. incognita</i> .....	47
<b>Figure 4.4(b):</b> An illustration of ten meta-modules from <i>M. incognita</i> merged co-expression network .....	50

## List of Tables

<b>Table 4.1:</b>	Summary of the identified modules: hub genes, module size, Top Enriched GO term, and Putative function identified in <i>Meloidogyne incognita</i> gene-gene co-expression network using Dynamic Tree Cut clustering method. ....	50
<b>Table 4.2:</b>	Putative biological functions of module hub genes identified in <i>Meloidogyne incognita</i> gene-gene co-expression network using g:Profiler.....	51
<b>Table 4.3(a):</b>	Abundantly expressed 3' regulatory motifs in the 10 modules in the Gene Co-expression network of <i>Meloidogyne incognita</i> identified using MEME suite web tool. ....	53
<b>Table 4.3(b):</b>	Abundantly expressed 3' regulatory motifs in the 10 modules in the Gene Co-expression network of <i>Meloidogyne incognita</i> identified using MEME suite web tool. ....	54

## List of Appendices

<b>Appendix A:</b>	Summary of 15 samples from five developmental stages of <i>Meloidogyne incognita</i> used in constructing a gene co-expression network, identify gene clusters, and discovery of regulatory motifs.....	91
<b>Appendix B:</b>	An illustration of a hierarchical clustered dendrogram using the Dynamic Tree Cut algorithm applied to the gene-gene co-expression network of <i>M. incognita</i> . One hundred and ten (110) modules are represented by the colour panel (Dynamic Tree Cut) in the x axis. ....	92
<b>Appendix C:</b>	A plot showing highly significant gene ontology terms in the darkslateblue module of the gene co-expression network of <i>M. incognita</i> . ....	93
<b>Appendix D:</b>	A plot showing highly significant gene ontology terms in the darkviolet module of the gene co-expression network of <i>M. incognita</i> . ....	94
<b>Appendix E:</b>	A plot showing highly significant gene ontology terms in the mediumorchard module of the gene co-expression network of <i>M. incognita</i> . ....	95
<b>Appendix F:</b>	A plot showing highly significant gene ontology terms in the mediumpurple1 module of the gene co-expression network of <i>M. incognita</i> .....	96
<b>Appendix G:</b>	A plot showing highly significant gene ontology terms in the navajowhite module of the gene co-expression network of <i>M. incognita</i> . ....	97
<b>Appendix H:</b>	A plot showing highly significant gene ontology terms in the plum module of the gene co-expression network of <i>M. incognita</i> .....	98
<b>Appendix I:</b>	A plot showing highly significant gene ontology terms in the blue module of the gene co-expression network of <i>M. incognita</i> . ....	99
<b>Appendix J:</b>	A plot showing highly significant gene ontology terms in the brown module of the gene co-expression network of <i>M. incognita</i> . ....	100

<b>Appendix K:</b>	A plot showing highly significant gene ontology terms.....	
	in the brown4 module of the gene co-expression network	
	of <i>M. incognita</i> . .....	101
<b>Appendix L:</b>	A plot showing highly significant gene ontology terms	
	in the darkseagreen3 module of the gene co-expression network	
	of <i>M. incognita</i> . .....	102

## List of Abbreviations

ARF	Adenosine diphosphate-ribosylation factor
BAK1	BRI1-associated receptor kinase 1 (BAK1)
CM	Chorismate mutase
CN	Cyst nematodes
CWDE	Cell wall-degrading enzyme
ETI	Effector-triggered immunity
GA	Gibberellic acids
MAMP	Microbe-associated molecular patterns
NAMP	Nematode-associated molecular pattern
NemChRs	Nematode Chemosensory GPCRs
NFS	Nematode feeding site
NILR1 receptors	NEMATODE-INDUCED leucine-rich repeat receptor-like kinase
NLR	Nucleotide-binding leucine-rich repeat
NPA	N-1-naphthylphthalamic acid
PAMP	Pathogen-associated molecular patterns
PCN	Potato Cyst Nematode
PDF	Pigment-dispersing factor
PDF-R	Pigment-dispersing factor (PDF) receptor
PPN	Plant-parasitic nematodes
PRR	Pattern recognition receptor
PTI	PAMP-triggered immunity
RKN	Root-knot nematode
SA	Salicylic acid
SSA	Sub-Saharan Africa
WGCNA	Weighted gene co-expression network analysis

## ABSTRACT

Plant-parasitic nematodes are a major cause of crop loss globally approximated at 150 billion dollars annually, and existing nematicides are toxic such that they offset the soil microbiome essential for crop growth. In order to develop eco-friendly mitigation tools, it is necessary to understand underlying molecular interactions driving the invasive phenotype of parasites. In this respect, a gene-gene co-expression network analysis of *Meloidogyne incognita* infecting *Solanum lycopersicum* was considered to be a good model for establishing a plant-nematode association. Transcriptomic data from five developmental stages of *Meloidogyne incognita* were obtained from the Sequence Read Archive (SRA) database of the National Centre for Biotechnology Information (NCBI). The data was pre-processed, generating a gene co-regulation count matrix. A systems biology tool, weighted gene co-expression network analysis (WGCNA) package, was used to describe gene correlation patterns across the development stages of *M. incognita*. The WGCNA tool was also utilised to detect clusters (modules) of highly correlated genes, summarise the modules using a module eigengene or an intramodular hub gene, connect modules, thus generating a gene-gene co-expression network of *M. incognita*. gProfiler tool was used to perform functional enrichment on module genes establishing biological function to established gene co-expression network clusters. Multiple Expectation maximizations for Motif Elicitation (MEME) suite web tool were used to determine each module's highly abundant regulatory motifs. A total of 30,894 most varied genes and ten (10) modules were identified to be expressed during a 6-week developmental process of *Meloidogyne incognita*. Genes within the blue, darkslateblue, and plum1 modules were significantly related to perception and response to abiotic and biotic factors. The brown module was associated with altering the host's transcriptional machinery. The darkseagreen3 module was responsible for producing peptide effector molecules facilitating parasite penetration into host tissues. The darkviolet and mediumorchard modules primarily facilitated the breakdown of organic substances withdrawn by the parasite from the host plant. A total of 10 hub genes, including Minc3s01527g24498, Minc3s02273g29200, Minc3s01418g23666, Minc3s01490g24232, Minc3s00044g02444, Minc3s00284g09370, Minc3s03424g33799, Minc3s02533g30509, Minc3s00002g00107, and

Minc3s00035g02069, were identified as potential biomarkers for diagnosis of *M. incognita*. Further, 10 unique regulatory motifs were identified as potential regulators of gene expression identified in the 10 modules. The results of this study provide new insights into the underlying molecular mechanism associated with interaction *M. incognita* and *S. lycopersicum*. This information will help in developing novel bioactive molecules targeting the regulatory motifs of *M. incognita*.

## CHAPTER ONE

### 1.0 INTRODUCTION

#### 1.1 Background Information

Plant-parasitic nematodes (PPN) are economically important pests that cause plant biotic stress and significant yield losses globally (Cox et al., 2019a). The control of PPN is considered more complex than other pests because they mostly live underground, where they attack plant roots. (Ali et al., 2018). The pathogenesis and symptoms caused by PPNs are non-specific, and often smallholder farmers are not aware of their associated losses or damages (Coyne et al., 2018). The global agricultural losses to PPNs are estimated at \$157 billion annually (Teillet et al., 2013). These losses do not account for the indirect losses associated with interactions with other pathogens such as bacteria and fungi (Srinivas et al., 2014).

Sedentary PPNs of the Meloidogynidae and Heteroderidae families inflict the most significant damage (Sato et al., 2019): the root-knot nematodes (RKNs) from the Meloidogynidae family and cyst forming nematodes (such as *Globodera rostochiensis*, *G. pallida*, and *Heterodera spp.*) from the Heteroderidae family. The RKNs transform root cells into specialized nematode feeding sites (NFS) (also known as giant cells) by inducing and reprogramming root cells to have repeated mitosis cycles without cytokinesis (Grunewald et al., 2009; Srinivas et al., 2014). The RKN consists of 100 known species distributed ubiquitously, and they affect a broad range of hosts estimated at 5000 plant species (Dahlin et al., 2019). *M. incognita*, *M. hapla*, *M. javanica*, *M. enterolobii*, and *M. arenaria* are the most destructive species of RKN that cause an estimated crop loss amounting to hundreds of billions of US dollars annually (Coyne et



al., 2018; Oزالvo et al., 2014). Economic losses caused by RKNs in Sub-Saharan Africa have not been estimated, yet it is a critical pest in many crops (Coyne et al., 2018).

The obligatory and sedentary RKN endoparasites depend on the host to develop and complete their life cycle. The parasitic nematodes alter host roots to form nematode feeding sites (NFS) to obtain a continuous supply of nutrients necessary for their development (Fitoussi et al., 2021). The parasite utilizes a needle-like apparatus known as a stylet to deliver effector protein secretions into root cellular structures, thus establishing and promoting an intimate interaction with the host. The effectors facilitate nematode root penetration, intracellular migration, establishment, and maintenance of nematode feeding sites. Effectors are synthesized predominantly by the oesophageal glands (one dorsal and two sub-ventral) (Iberkleid et al., 2013). Other organs that secrete effectors are amphids and cuticles. Released protein effectors are major virulence determinants mediating biochemical, molecular, and morphological changes in infected host cells and tissues (Fitoussi et al., 2021; Oosterbeek et al., 2021). Of various effector categories, some secreted nematode effectors have been found to either modify host cell wall structure, mimic activities of host proteins, manipulate host developmental pathways to their advantage, subvert defence signals, and target and recruit host post-translation required for defense signaling and immune responses (Hewezi, 2015; Rodiuc et al., 2014). Successful characterization and isolation of multiple effectors of plant-parasitic nematode species have been made possible by genome, transcriptome, proteome, secretome, and RNAi approaches (Bellafiore et al., 2008; Sato et al., 2019).

Despite challenges faced by asexual organisms surviving in diverse conditions, the asexual *M. incognita* has evolved to adapt in diverse environments, highly invasive and polyphagous compared to other sexually reproducing plant pests (Blanc-Mathieu et al., 2017). An estimated cost of 80 million is spent yearly to manage *M. incognita* (Hewezi, 2015). The use of resistant crop varieties and planting of clean planting material are some of the strategies employed to control *M. incognita*. However, *M. incognita* is presently controlled using chemical pesticides in large-scale commercial farming, which is toxic to humans and the soil microbiome hence the need for creating environmentally friendly mitigation measures.

The molecular mechanisms that facilitate successful plant-nematode association of *M. incognita* are not fully deciphered. This study focused on understanding plant-nematode association at the molecular level to generate novel approaches for mitigating *M. incognita*. Construction and identification of modules in the gene-gene co-expression network inferred key biological functions facilitating parasitism. The gene-gene co-expression network analysis established modules facilitating host defences subversion, targeting host post-translation, and mimicry of host proteins. Significant 3' UTR motifs promoting the nematode's invasiveness were determined as novel candidates for drug targeting.

## **1.2 Statement of the Problem**

The root-knot nematode, *M. incognita*, is rendered a scientific and economic important parasite since it contributes to global crop losses estimated to be between \$80 billion to \$157 billion annually (Teillet et al., 2013). The United States alone incurs an annual

agricultural loss of \$10 billion to PPN nematode is higher in comparison to invasive insect losses of \$6.6 billion (Coyne et al., 2018).

In Sub-Saharan Africa, *M. incognita* is a major parasite of several crops, including vegetables, fruits, and legumes. Up to 80% of yield losses are estimated to be caused by *M. incognita*, which can have a devastating impact on the livelihoods of smallholder farmers who rely on these crops for food and income (Santos et al., 2019). Surveillance studies conducted in Kenya show that *M. incognita* is a major parasite of several crops, including tomato, sweet potato, maize, pepper, and cowpea (Cox et al., 2019b). In tomatoes, for example, *M. incognita* causes yield losses of up to 70%, leading to significant economic losses for farmers. Moreover, *M. incognita* limits the main food crops in Sub-Saharan Africa and has serious implications for food security and the overall well-being of the population (Akinsanya et al., 2020). *M. incognita* also affects the quality of crops. For example, in tomatoes, the nematode infection can lead to fruit malformation, reduced size, and poor coloration, which can make the produce less marketable and therefore less profitable for farmers (Santos et al., 2019). It is therefore important to develop effective and sustainable strategies for managing *M. incognita* to minimize its impact on crop production and livelihoods in the region. The *M. incognita* is a parthenogenetic or apomictic organism since it reproduces asexually (McCarter et al., 2003). Although organisms reproducing asexually have less ability to survive in diverse environments, *M. incognita* has emerged to be very successful. The phytoparasite affects approximately 5,500 plant species, including arable agricultural and horticultural crops (Zhang et al., 2016). *M. incognita* is distributed globally, demonstrating high specialisation, adaptability, and variability (Cox et al., 2019a). The parasitic nematode has the ability to evade host immunity and existing mitigation

strategies. Also, it creates co-infection dynamics with bacteria, fungi, and viruses resulting in disease incidents among arable crops and forest vegetation (Xiong et al., 2015). Chemicals remain the efficient way of controlling RKN. However, synthetic nematicides pose safety concerns to public health and the environment (Xiong et al., 2015). Furthermore, there is a limitation of knowledge on gene interactions and key genes driving the development and virulence of *M. incognita*.

### **1.3 Research Question**

Can weighted gene co-expression network analysis depict genes interactions in different developmental stages of *Meloidogyne incognita*?

### **1.4 Study Objectives**

#### **1.4.1. General Objective**

To generate a gene co-expression network to identify key genes involved in the development of *Meloidogyne incognita*.

#### **1.4.2. Specific Objectives**

- i. To develop a weighted gene co-expression network, identify modules and hub genes that mediate the development of *Meloidogyne incognita*.
- ii. To establish functions of the identified modules and hub genes in the weighted gene co-expression network of *Meloidogyne incognita*.
- iii. To identify 3'-untranslated regions (UTRs) that regulate the development of *Meloidogyne incognita*.

## **1.5 Justification of the Study**

Due to inefficiency in mitigation strategies, *M. incognita* is the leading cause of crop loss among small-holder and large-scale farmers (Cortada et al., 2019). Some of the mechanisms used by *M. incognita* to reduce the crop growth index include subverting host defense signals and targeting host post-translation required for defense signaling and immune responses (Coyne et al., 2018). An in-depth understanding of the host-parasite interaction is critical in deciphering integral biological processes driving its virulence, alteration, and mimicry of host factors-signaling molecules, the resistance of existing mitigation strategies, and the establishment of permanent feeding sites. Establishing knowledge of host-parasite interaction will help develop novel mitigation strategies that promote good environmental conditions for plant and soil microbiome.

## CHAPTER TWO

### 2.0 LITERATURE REVIEW

#### 2.1 Nematodes

Nematodes are worm-like microscopic and eukaryotic organisms that are part of the fauna, and they are found in diverse habitats ranging from terrestrial, aquatic, optimal to extreme environs (Rashidifard et al., 2019). Nematodes rely on humidity, moisture, or a film of water for survival and activity. Most nematodes reside in the soil, and they are divided into five trophic groups including: bacterial feeder, fungal feeders, herbivores, omnivores, and predators (Vinciguerra, 1979). First, bacterial feeding nematodes suck bacteria suspensions from water films, surfaces, and soil organic matter. The bacteria feeders feed on colonies leading to the continuous replenishing of new bacteria involved in decomposition (Sánchez-Moreno et al., 2010). Also, the bacterial feeders help in nitrogen-fixing since they transfer and inoculate rhizobia on legume plant roots. Second, fungal feeding nematodes can insert their stylets and suck out the content of fungal hypha (Monokrousos et al., 2021). Previous studies have associated fungal feeding nematodes with reducing the soil burden of pathogenic fungi and oomycetes such as *Fusarium*, *Pythium*, and *Rhizoctonia* (Langat et al., 2008). Third, omnivore nematodes are known to depend on several food sources since they feed on fungal hyphae, algae cells, oligochaete eggs, and other nematodes (Ferris et al., 2012). The feeding stylet is spear-shaped and has a wider aperture for feeding. Fourth, Predator nematodes have an open cavity with a specialised tooth for capturing and consuming nematodes and other microscopic animals (Langat et al., 2008). Lastly, herbivorous nematodes have a hypodermic-spear like stylet for feeding and sucking cells of the plant roots. Approximately 20 to 25 different genera of nematodes have

been identified, and most of them have different host preferences (Kanfra et al., 2018). The herbivorous nematodes form the economically significant plant-parasitic nematodes (PPNs) with different parasitic strategies and behaviours.

Nematodes that are not plant-parasitic, such as bacterial feeders, predators, and fungal feeders, are called free-living nematodes (Kanfra et al., 2018). The free-living nematodes play an essential role in influencing microbial diversity, nutrient cycling, digesting consumed microbial biomass to release  $\text{NH}_4^+$  utilised by plants, and dispersing and inoculating essential bacteria on plant roots (Majdi & Traunspurger, 2015). The high abundance of free-living nematodes is an indicator of healthy soil free from pathogenic microbes and nematodes.

## **2.2 Nematodes of Economic Significance**

Approximately 48 percent of the nematode species have been found to parasitize on plants and animals, making them of economic importance. Parasitic nematodes are known to cause disease in plants, animals, and humans (Rashidifard et al., 2019). Plant-parasitic nematodes (PPNs) are diverse and dwell on foliage, stems, or roots depending on the species (Vieira & Gleason, 2019). Plant-parasitic nematodes of agronomic significance attack below ground plant tissue; globally, PPN cause an annual estimated loss of over \$157 billion (Kaloshian & Teixeira, 2019; Teillet et al., 2013). Annual agricultural losses of \$10 billion in the United States have been linked to nematodes compared to insect losses of \$6.6 billion (D. Coyne et al., 2018; Y. Zhang et al., 2016). In Sub-Saharan Africa (SSA), an estimated \$70 million of potatoes is lost to Potato Cyst Nematode (PCN), *Globodera rostochiensis* (D. Coyne et al., 2018). Despite their impact in agriculture, there exists no reliable data to quantify the impact of RKN despite it being considered the world's most voracious plant pathogen (Rutter et al., 2015). The

root-knot nematode affects a wide range of vegetative propagated plants crops (such as potatoes and yams), staple food (such as maize and rice), horticultural crops (such as guava and roses) and cash crops (such as cotton, tea, and coffee) (D. Coyne et al., 2018). Usually, the *Meloidogyne species* cause roots to form galls rendering them unable to effectively uptake water, minerals, and nutrients leading to stunting (Bernard, 2017). Also, RKN infection compromises plant immunity resulting in co-dynamic infection of either bacteria, fungi, or viruses. Small-holder farmers in Sub-Saharan Africa have limited ability to diagnose and apply relevant mitigation strategies (Cortada et al., 2019).

### **2.3 Taxonomy of Plant Parasitic Nematodes**

According to Kaloshian and Teixeira (2019), a total of 4,100 PPN species have been identified and classified into: endoparasites, semi-endoparasites, or ectoparasites. The classification is based on their location on the host while feeding (Siddique & Grundler, 2018). Endoparasites are further divided into either migratory or sedentary depending on motility behavior after establishing feeding sites in the host (Hassan et al., 2010). The continuous migration of endoparasites causes severe necrotic damage as they feed and migrate inside plant tissues (Shah et al., 2017). The endoparasites causing necrosis include spiral nematode (*Helicotylenchus* spp.), lance nematode (*Hoplolaimus* spp.), lesion nematodes comprising of *Pratylenchus* spp. and *Scutellonema* spp., burrowing nematodes associated with *Radopholus* spp., pine wilt nematode (*Bursaphelenchus xylophilus*), red-ring nematode (*Bursaphelenchus cocophilus*), and rice root nematode (*Hirschmanniella oryzae*) (D. Coyne et al., 2018). Sedentary endoparasites include nematode groups which are intensely studied, the root-knot nematode (RKN) (*Meloidogyne* spp.) and cyst nematodes (CNs) (of genera *Globodera* and *Heterodera*)



penetrate and form an intimate relationship with the plant host after penetration. However, RKNs and CNs differ in their migration modes and the formation of specialized feeding sites (Xiong et al., 2015). The RKNs penetrate the roots mainly at the root elongation, move intracellularly, and induce the establishment of permanent feeding sites, and become sedentary. In contrast, CNs penetrate at undefined root locations, move intracellularly, degrade cell walls forming enlarged multinucleated cells (known as syncytia), and become sedentary (Kaloshian & Teixeira, 2019).

Most life-forms that reproduce asexually are known to have less ability to survive in diverse and adverse environments (Mccarter et al., 2003). However, details of how a parthenogenetic root-knot nematode (RKN) has high adaptability, distributed globally under different ecological conditions, affecting over 5,500 plant species, is scarcely known (Dahlin et al., 2019). The parasitic success of RKN is linked to the effectors it releases, manipulating the host's physiology and immunity response (Cox et al., 2019a). Understanding gene expression patterns, interaction profiles and conserved regulatory motifs facilitating RKN's life cycle and parasitism will provide insights into its regulation (Zhang et al., 2016).

#### **2.4 The *Meloidogyne* genus**

The *Meloidogyne* genus, also known as root-knot nematodes (RKN), are important obligate and sedentary PPNs (Cetintas et al., 2018). Approximately 100 species of *Meloidogyne* have been identified to date, with *Meloidogyne arenaria*, *M. chitwoodi*, *M. enterolobii*, *M. exigua*, *M. hapla*, *M. incognita*, *M. graminicola*, and *M. javanica* being the dominant species of RKN affecting crops of agronomic significance (Isagie et al., 2018; Kumar et al., 2019). The eight species are distributed globally, affecting more than 5500 plant species, of which *M. incognita* causes the highest parasite burden

(Dahlin et al., 2019). *M. incognita* is a parthenogenetic organism reproducing asexually (Serenio et al., 2019). Mostly, parthenogenetic organisms have difficulty adapting to both diverse and challenging environmental conditions (Szitenberg et al., 2017). Despite these challenges, *M. incognita* is widely distributed across the continent, demonstrating a high level of specialization, adaptability, variability and high reproduction of approximately 1000 clonal populations from a single female (Cox et al., 2019a). In addition, the nematode is polyphagous, can evade hosts immunity, and is resistant to current mitigation strategies (Coyne et al., 2018). Previous studies have utilized both coding and non-coding mRNA to investigate the behavior and molecular basis of *M. incognita* in host selection and invasiveness (Id et al., 2019). Studies have established that the entire genome of *M. incognita* consists of 50 percent gene duplicates (Blanc-Mathieu et al., 2017; Medina et al., 2018). In addition, the duplicate genes exhibit variations that are attributed to the rich presence of transposable elements. The copy number variants (CNVs) infers the differential capacity of avirulent or virulent *M. Incognita* (Blanc-Mathieu et al., 2017; Serenio et al., 2019). Understanding the system biology of *M. incognita* will play a critical role in the development of efficient control strategies (Szitenberg et al., 2017).

## **2.5 The lifecycle of Meloidogyne species**

The life cycle of the genus *Meloidogyne* has two distinct phases, the exophytic and endophytic phases. In the exophytic phase, the nematode is motile and usually looking for a host, while in the endophytic phase, it develops an intimate parasitic relationship with respective host plants (Dubreuil et al., 2007). *Meloidogyne* spp. has five developmental stages: the zygote (egg), four juvenile (larval), and adult stages. The zygote undergoes embryonic development forming a first vermiform stage, juvenile

(J1), with or without the influence of plant exudates. The J1 moults into a second-stage juvenile (J2), with an approximate length of 400  $\mu\text{m}$  and a width of 15  $\mu\text{m}$  (Figure 2.1). Hatching of the vermiform J2s is triggered by exudates released by plant roots (Ali et al., 2018). The J2 stage is the only infective and motile stage capable of penetrating root tissue, and it is also referred to as pre-parasitic J2 (ppJ2). The ppJ2s contain sufficient lipid reserves to use as sources of energy as they seek a host (Da Rocha et al., 2021).

The ppJ2s are attracted to root exudates and formed concentration gradients around host plants (Goyena, 2019). The ppJ2s migrate toward the host root system and penetrate the root destroying epidermal cells. The success of root penetration is made possible by a combination of enzymatic and mechanical disruptions (Vieira et al., 2011). The infective stage secretes the cell wall degrading and modifying enzymes from the secretory gland via a syringe-like stylet. The nematode migrates from the cortical cells via the vascular cylinder to the root elongation zone (Jaubert et al., 2005). Upon reaching the root tip, the ppJ2 secretes effector proteins and other molecules that induce the formation of approximately five to seven multinucleated and hypertrophied giant cells. The giant cells are the sole source of nutrients for developing endoparasites and is thus also called permanent feeding site. Giant cells are characterised by being metabolically hyperactive and dividing without cytokinesis (Kumar et al., 2019). Local cell walls thickening, cytoskeleton reorganisation, vacuoles fragmentation and numerous mitochondria are the special features associated with giant cells (Mejias et al., 2019).

The ppJ2s uptake nutrients from the established permanent feeding site through the stylets and rapidly develop into sedentary third (J3) and fourth (J4) juvenile stages. The

later stages are morphologically difficult to distinguish and need a thorough examination of the stylet and superimposed outer cuticles. Usually, as the nematodes advance, the prominence of the stylet diminishes, and the size of superimposed outer cuticles increases (Da Rocha et al., 2021). Finally, stage four juveniles develop into adult males and females with marked morphological differences (Figure 2.1). The adult male returns into a vermiform morphology and do not participate in sexual reproduction of obligate parthenogenetic *Meloidogyne* species progeny. Male root-knot nematodes populations are extremely rare and have no evidence of parasitism (Gheysen & Fenoll, 2002). However, extreme environmental conditions result in high proportions of males compared to females (Jaubert et al., 2005). Adult females remain sedentary; their functional stylet and pear-shaped morphology distinguish them from adult males. The females resume feeding, produce and extrude hundreds of eggs in a glycoproteic gelatinous mass on the root surface (Moens, 2015). The life cycle is complete as viable eggs eventually hatch by the influence of host-root exudates forming the next generation of parasitic juveniles (Da Rocha et al., 2021). The root-knot nematode's parasitic cycle is characterised by distinct stages that have profound morphological and functional differences.

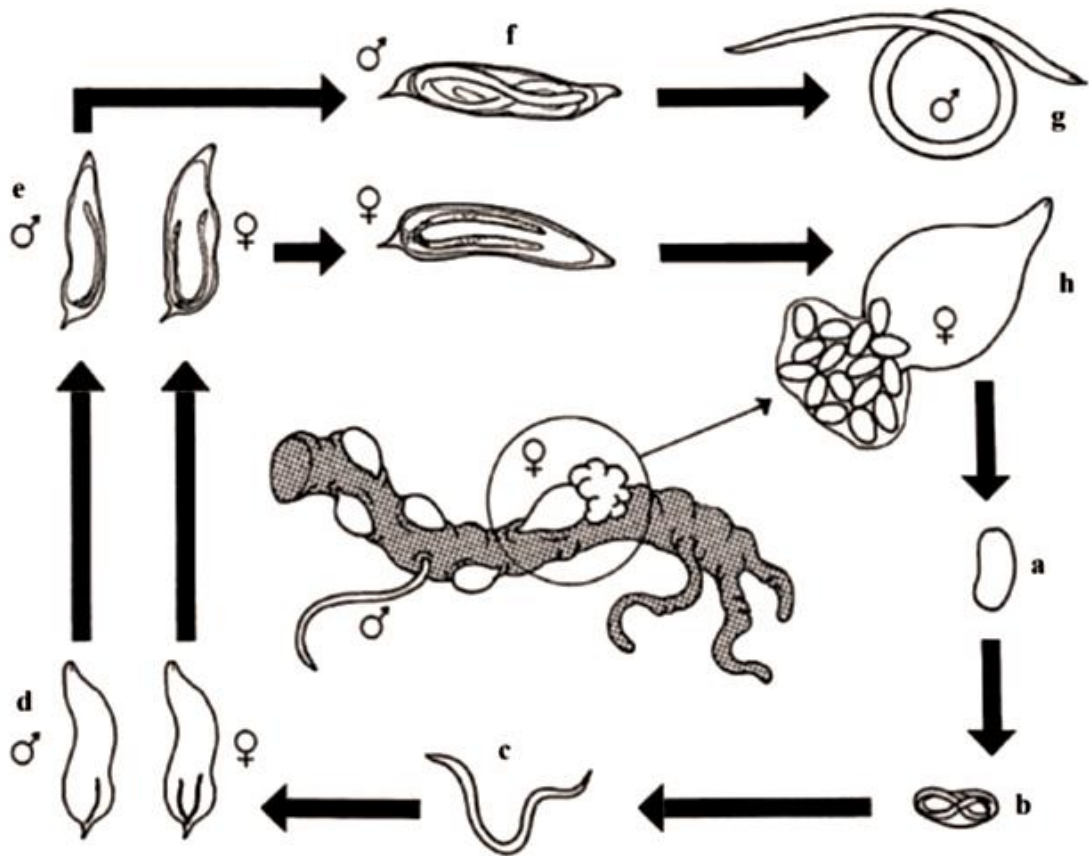


**Figure 2.1:** The five developmental stages of genus *Meloidogyne*

Figure 2.1 is such that a=zygote; b= first vermiform juvenile; c = second juvenile; d= swollen, second juvenile; e= swollen, third sedentary juvenile; f= swollen, fourth sedentary (male and female) juvenile; h=swollen, sedentary female with eggs (Illustration adapted from Moens, 2015).

## 2.6 Diagnosis and prevention of *Meloidogyne incognita* Infestation

Root-knot nematodes cause roots to form galls which significantly curbs the uptake of water and mineral salts and nutrients from the soil (Hu et al., 2020). The morphological changes cause the manifestation of stunting, chlorosis, premature leaf dropping, and wilting of plants mistaken to be nutrition deficiency and viral infection. Diagnosis of the RKN species helps in determining mitigation strategies (Poveda et al., 2020).

Nematode morphological and morphometric characteristics are the main features for distinguishing different root-knot nematode species and developmental stages (Moens, 2009). The perennial morphological patterns of adult females are mostly utilized to establish interspecies differences (Ntidi et al., 2019). However, the existing intraspecies variations and interspecies overlaps within the *Meloidogyne* genus make it difficult to classify to species level. The rise of *Meloidogyne spp.* incidents over the years have resulted in the combination of molecular techniques with morphological and morphometric measurements (Fourie et al., 2019). Molecular approaches have proven accurate in distinguishing *Meloidogyne species* by using ribosomal DNA (rDNA), mitochondrial DNA (mDNA), and sequence characterized amplified regions, and randomly amplified polymorphic DNA. Ribosomal DNA characterization is mainly utilized to distinguish the parthenogenetic species in the genus *Meloidogyne* (Rashidifard, Marais, et al., 2019).

Mostly, RKN control measures focus on reducing the nematode numbers, and they include (i) application of organic matter to lower the pH and increase the population of free-living nematodes. The free-living nematodes are as flora bacteria to pathogenic bacteria on human skin or gut; therefore, they control the RKN population density (Westphal, 2011). (ii) Growing cover crops such as *Brassica species*, Marigolds, and Sudan grass produce chemicals antagonistic to PPNs. Studies have established that isothiocyanate and glucosinilate chemical compounds of *Brassica species* mitigate many RKN species (Poveda et al., 2020). In addition, cover crops are used to make soil compost, form stable soil amendments, and boost soil normal flora such as free-living nematodes (Karuri et al., 2017). Also, intercropping of plant species resistant to *M. incognita*, for instance, *Crotalaria spectabilis* and *Mucuna pruriens L.*, help in

minimizing the parasitemia. (iii) Crop rotation practices prevent the build-up of parasitic nematodes. However, root-knot nematode has a wide range of hosts, thus difficult to control using the rotation method (Jones et al., 2013). (iv) Soil sterilisation using solar energy has shown potential in controlling soil-borne pathogens such as RKNs. For solarisation to be effective the field is ploughed during the hottest months such that the soil is loose and has adequate moisture; the soil is airtight sealed for 45 days. (v) In farmland regions having plenty of water, the area can be flooded with water to eliminate the nematodes. In the case of rice cultivation, flooding conditions helped a significant reduction of the root-knot nematode (Bernard et al., 2017). Intercropping with cultivars that favor bare fallowing and flooding have respectively shown to be a success in reducing soil nematode population. (vi) Growing varieties of crops with known resistance to nematodes (De Medeiros et al., 2017). For instance, growing *S. lycopersicum* (tomato) with a single dominant resistant gene (Mi-1) produces more yields despite farm infestation with root-knot nematodes (El-Sappah et al., 2019). (vii) Ensuring the use of clean planting material and sanitisation of farming tools, fields, and greenhouses significantly lower the PPNs. Usually, the planting material (such as rhizomes and tubers) are treated for twenty (20) minutes before planting (D. L. Coyne et al., 2013). For instance, *Scutellonema bradys* and *Radopholus similis* affecting yams and bananas, respectively, have greatly been controlled by hot water treatment (Mathew & Opperman, 2020). (viii) Use of ethanolic biological nematicides extracted from *Eucalyptus citriodora*, *Azadirachtin indica* (neem), *Withania somnifera*, and garlic formulation to prevent progression of infective juveniles (Lynn et al., 2010). (ix) *Meloidogyne incognita*, a soil nematode, is subject to fungal and bacterial infections (Cetintas et al., 2018). Many microorganisms studied in the last decade have shown

great potential for controlling soil helminths. *Arthrobotrys oligospora*, *Bacillus spp.*, *Burkholderia cepacia*, *Paecilomyces lilacinus*, *Pasteuria penetrans*, *Pseudomonas spp.* and *Purpureocillium lilacinum* are some of the biocontrol microorganisms (Osman et al., 2018). The mechanism of action of biocontrol microorganisms is such as inducing host systemic resistance and production of nematicidal toxins (Xiong et al., 2015). For instance, *P. lilacinum* colonizes the zygote (egg) shell, juvenile cuticle, or hyphal penetration of the *M. incognita*, thus influencing plant growth from pre-plant to plant vegetative phases (Seo & Kim, 2014). Also, *Bacillus pumilus*, *Bacillus subtilis* and *Bacillus thuringiensis* produce crystalline proteins, which are toxic to *M. incognita*, thereby enhancing plant health (Osman et al., 2018).

## **2.7 Plant-Nematode Interaction**

Plant-parasitic nematodes induce several signalling pathways when interacting with host plants through nematode associated molecular patterns (NAMPs) (Poveda et al., 2020). Also, nematode secretions activate different plant genes while establishing nematode feeding sites in the host (Abd-elgawad, 2021). The host plants detect the NAMPs and nematode secretions, thereby activating the basal immune system to prevent nematode invasion. Usually, the nematodes secrete effector proteins that circumvent the basal defences by inducing changes in the host physiological process, such as cytokinesis, signalling pathways, and posttranscriptional processes (Pulavarty et al., 2021). In this section, we explore signalling events involved in plant nematode interaction.



### **2.7.1 Host finding: Root-Knot nematode Attraction to the host**

Host finding is the first signaling event of the infective pre-parasitic second juveniles' (ppJ2) survival and progeny progression through plant-parasite interaction (Tran et al., 2016). The ppJ2 moves towards the host roots through chemotaxis mediated by host plant root exudates (Ali et al., 2018). In the absence of host resistance responses such as callose deposition and reactive oxygen species (ROS), the ppJ2 enter the root cells and locate the vascular tissues where they initiate nematode feeding sites (NFS) (Kaloshian & Teixeira, 2019). The ppJ2 source nutrients from the NFS needed for their development through their subsequent sedentary life stages (Teixeira et al., 2016). The ppJ2 secrete effectors containing cell wall-degrading enzymes (CWDEs), transcription factors (TFs), and virulence proteins (Avr proteins) to initiate the NFS. Parasitism is achieved when the secreted effectors interact with host genes and proteins to trigger the differentiation of host root cells into feeding cells and suppress defense responses (Ali et al., 2018).

A study by Tran et al., (2016) utilized an artificial 3-dimensional soil matrix of Pluronic F-127 to mimic and recreate cues necessary for RKN attraction to the plant root tip. Cues such as plant hormones, pH gradient, and genetic diversity of the RKN species play key roles in infective juvenile's chemotaxis towards the roots (Kaloshian & Teixeira, 2019). From the study, high ethylene concentrations lowered RKN and *Heterodera glycines* populations in Arabidopsis but enhanced the attractiveness of the roots to *H. schachtii*. Second, matrix regions of low pH attracted the infective juveniles (Tran et al., 2016). Lastly, the experiment showed that different RKN species moved towards the host's roots at varying rates, signifying gene expression variance among RKN species (Kaloshian & Teixeira, 2019). Understanding signaling pathways

associated with PPN chemotaxis and attraction to host roots is the hallmark for developing novel control tools.

### **2.7.2 Establishment of feeding sites and adaptation of Neoplastic Feeding Sites**

The parasitic nematode heavily relies on nutrients and solutes derived from the host plant to develop whilst reducing agronomic yield due to pathological disturbance of photosynthetic and metabolic products diversion (Siddique & Grundler, 2018). The RKN secretes a barrage of effectors that stimulate karyokinesis of the nematode feeding site (NFS) cells without cytokinesis, resulting in giant cell (GC) formation (Sarde et al., 2018). High metabolic activity and cell division of giant cells result in large galls on the roots (Hassan et al., 2010; Kumar et al., 2019).

Neoplastic feeding site formation causes remarkable transcriptional, metabolic, and structural transformation in host plant physiology. Transformation of NFS morphology and physiology results in sink tissues catering for nematode developmental needs (Perfus-barbeoch et al., 2012). The NFS cells are highly specialized, consisting of dense cytoplasm containing numerous organelles composed of the Golgi apparatus, mitochondria, ribosomes, plastids, smooth endoplasmic reticulum, and numerous small vacuoles. The ability of NFS to translocate nutrients is increased by the interface of cells wall ingrowths the xylem (Bellafiore et al., 2008).

### **2.7.3 Alteration and Mimicry of host factors-signaling molecules**

Plant-parasitic nematodes produce phytohormones essential in cell division modulation, altering auxin pathways, molecular mimicry of plant factors, using the host posttranslational machinery, and subverting defense signaling (Hewezi, 2015). Cytokinins, auxins and gibberellic acids (GA) are the main phytohormones produced

by PPNs. Cytokinins and auxins are vital in activating the cell cycle and influencing the feeding site and neighboring cells, therefore playing a key role in expanding the giant cells. Comparative analysis of sedentary PPNs has shown high levels of cytokinins produced by RKNs compared to cyst nematodes (CN), signifying the presence of cytokinin-synthesizing genes. Studies have also revealed that *M. incognita* influences auxin genes' expression by targeting the PIN group of genes and specifically the auxin transport proteins. However, the intricate control of auxin flow is not well known (Hassan et al., 2010).

Chorismate mutase (CM) enzymes are among the effector groups that influence the feeding and lifestyle of *M. incognita*. The CMs catalyse the shikimate pathway, leading to chorismate, a precursor of auxin formation, phytoalexins, flavonoids, indole-3-acetic, and lignin (Hassan et al., 2010). In addition to cell differentiation and division, CM also suppresses the host immunity defense compounds such as salicylic acid (SA) and flavonoids. Previous studies have shown that treatment of RKN target host plants with N-1-naphthylphthalamic acid (NPA), a polar auxin transport inhibitor, reduces the host's susceptibility to RKN (Hassan et al., 2010). Also, gibberellic acids (GA) (also referred to as gibberellins) of the tetracyclic diterpenoid family are produced, and they regulate growth and developmental processes in host plants. The infection of RKN leads to GA<sub>12</sub>, a specific GA, at the infection site. High concentrations of GA suppress host defenses regulated by jasmonic acid (JA). However, the GA's has been linked to high reliance on auxin transport.

#### **2.7.4 Role of microRNAs (miRNAs) in Plant-Nematode Interactions**

Plant small RNAs regulate various gene expression processes such as development response to either abiotic stress, hormonal signalling, metabolism, symbiotic microbes,

or parasitic microorganisms (Marteu et al., 2017). Plant small RNAs are classified into microRNAs (miRNAs) and small interfering RNAs (siRNAs). Transcription of miRNA genes by RNA polymerase II produces an RNA precursor of a double-stranded RNA hairpin in structure. The RNA precursor, also known as pri-miRNA, is processed by DICER to generate a secondary RNA precursor known as the pri-miRNA and a 20-22 nucleotide long miRNA duplex. The mature miRNA of the duplex is incorporated into the RNA-induced silencing complex (RISC) protein. The RISC protein, ARGONAUTE1 (AGO1), binds to and guides the mature miRNA based on sequence complementarity to bind with a targeted messenger RNA (mRNA) its degradation or translation inhibition.

The significance of microRNAs (miRNAs) influencing transcriptomic shift and changes during neoplastic feeding site formation is widely documented (Marteu et al., 2017). The microRNAs are small non-coding RNAs that regulate gene expression by binding to their respective target messenger RNA (mRNA). Binding to target mRNA leads to degradation, thus repressing translation or transcriptional activity. Mechanism of transcriptome reprogramming by miRNA families during giant cell formation by targeting transcription factors. For example, *miR159* and *miR319* (host miRNAs) have been shown to play a role in giant cell formation in Arabidopsis and Tomato, respectively, by regulating the expression of its target transcription factors MYB33 and TCP4, respectively (Zhao et al., 2015). Constitutive upregulation of *miR159* and *miR319* expression has been shown to reduce susceptibility to *M. incognita*, while reduced *miR519* and *miR319* increase its susceptibility.

Similarly, overexpression of the modified version of MYB33 and TCP4 (target mRNAs produced by nematodes) that cannot be cleaved by *miR519* and *miR319*, respectively,

leads to increased susceptibility to RKNs. Notably, transcriptome analysis of MYB33 overexpression lines showed that it controls 16.6% of the GC transcriptome, indicating the role of the *miR519*-MYB33 regulatory system in gene expression modulation during RKN parasitism. Mechanisms of how RKN utilizes mRNA to manipulate the host have been uncovered. However, the mode of action of nematode miRNAs remains unexplored.

### **2.7.5 Plant-Parasitic Nematode Effectors and Host interactions**

Nearly 500 *Meloidogyne spp.* proteins have been identified to alter signaling pathways (Teillet et al., 2013). Effectors are proteinaceous signaling molecules secreted by PPNs to target important host molecular components to facilitate parasitism. The effectors have evolved, and an estimate of 60 encoding genes linked to them have been discovered (Vieira et al., 2011). The signaling molecules degrade host cell walls or modulate host development pathways to induce and maintain the feeding sites. The effectors also modify the host defense response to inhibit host infection-counter mechanisms (Melillo et al., 2006; Vieira et al., 2011). Inexpensive next-generation sequence technology has facilitated the discovery of PPN species effectors. There is a continuous discovery of diverse effector genes classified into large gene-effector families due to PPN species diversity and plant host selection pressure. Comparative genomics studies have shown that effector repertoires differ between nematode species. In addition, studies have been done to predict new putative effectors and/or promoters preceding effector gene sequences. Nevertheless, there have been limited studies aimed at determining effector functions and parasitism competence by knocking out effector genes.

Studies have revealed that the RKN secretes a repertoire of effectors that mimic host signaling, regulate host gene expression, or interact with host-specific proteins (Hassan et al., 2010; Vieira et al., 2011). The infective juvenile has been shown to secrete enzymes that enable them to penetrate and transverse through the host cells. The proteins consist of enzymes, such as;  $\beta$ -1,4-endoglucanase, pectate lyase, that break down and soften polygalacturonate, pectin, cellulose, and other cell wall components host cells (Hassan et al., 2010; Jaubert et al., 2005; Molinari & Miacola, 1997). Also, cellulose-binding proteins or chaperones are simultaneously secreted with enzymes, thus accelerating cell wall digestion. The chaperone improves the efficiency and speed at which the invasive J2 penetrates, moves through host roots, and efficiently feed on the cells (Hassan et al., 2010; Jaubert et al., 2005).

*Meloidogyne incognita* mimics plant signaling peptides that induce plant growth and development by manipulation of signaling pathways. For instance, C-Terminally Encoded Peptide (CEP) effector increases the host nitrogen uptake and regulation of NFS size. Also, CLAVATA-like effectors (CLE) are recognized by host CLE-receptors and modify host developmental signaling pathways to promote feeding site formation. Studies have shown that some PPN effectors are obtained via horizontal gene transfer (HGT). For example, IDA-like effectors that act as cell wall modifying enzymes have been discovered. The IDA-like effectors mimic plant-signaling peptides that control floral organ abscission and lateral root emergence. Glutathione synthase (GS) genes are responsible for housekeeping enzyme that protects cells against redox stress. Orthologs of the GS genes are, 3ODO8 gene in several PPNs (including RKN), 1OAO3 in *Heterodera schachtii* and Hs32EO3 in cyst nematodes. The GS genes express

mechanistic effectors that manipulate host gene expression by modulating epigenetic means and targeting host transcriptional machinery to alter susceptibility.

*M. incognita* effectors also bind to the host's transcription factors, thus activating expression. *M. incognita* secretes effector Mi16D10, containing CLE-like domains/motifs (Kiyohara & Sawa, 2012). Effector Mi16D10 targets the nuclei of the host cells by interacting with SCARECROW-like transcription factors (Rutter et al., 2015). Targeting the nuclear results in transcription control, which is vital for developing feeding sites and alienation of defense mechanisms (Jaouannet & Rosso, 2013). Short root transcription factors (SHR) depend on the SCARECROW transcription factors as a source of precursors for their action. In addition, SCARECROW transcription factors involve endoderm differentiation and root radial patterning, which are critical for the maintenance of feeding sites (Mejias et al., 2019).

Some of the root-knot nematode's effectors are essential in the modulation of the host physiology. For instance, the 14-3-3 effector bind with chaperones preventing the host defence signals from initiating lysis of irregular intercellular cells distributed in the nematode feeding sites. Calreticulin (CRT) also enhances protein maturation and calcium homeostasis. Calcium homeostasis is vital in maintaining the GC by sustaining intercellular trafficking and cell adhesion (Hassan et al., 2010). Calmodulin (CaM), calcium-dependent protein kinase (CDPK1), and translationally controlled tumor proteins (TCTPs) effectors control cell expansion, mitosis and cell wall synthesis pathways (Hassan et al., 2010).

## **2.8 Cellular immune response in plants**

Plant immune systems have evolved to detect and fight viral, bacterial, fungal, and nematode infections (Lin et al., 2016). Usually, the process by which the plant perceives nematode penetration is made possible by collecting intracellular and extracellular receptors localized in the host root cell (Phong et al., 2014). Usually, the invading pathogen encounters multi-layered defense responses generated by the host. In the plant, the cell wall is the first physical barrier faced by pathogens (Shah et al., 2017). Once the pathogen penetrates or overcomes the cell wall, the host cytoplasm serves as the second level of defense. Next to the cell wall, the cell membrane consists of localized ligand-binding transmembrane proteins known as pattern recognition receptors (PRRs) (Fitoussi et al., 2021). The PRRs often recognize conserved microbe or pathogen-associated molecular patterns (MAMPs/PAMPs) such as cell wall derivatives, carbohydrates, lipids, and proteins (Bellafiore et al., 2008). Recognition of MAMPs/PAMPs by the PRRs initiates a downstream cellular signaling cascade called PAMP-triggered immunity (PTI) in the host cells' cytoplasm (Sato et al., 2019). In response to MAMP detection, activation of the mitogen-activated protein kinases (MAPKs), production of reactive oxygen species (ROS), and activation of defense signaling pathways occur via jasmonic acid (JA) and salicylic acid (SA) (Hewezi, 2015). PTI-triggered immunity is usually successful in protecting the plant against non-adapted microbes. Some pathogens successfully gain access to the host cell by releasing effectors that interfere with the PTI compromising the host basal defense system (Lin et al., 2016). However, the microbe might further activate the host's intracellular nucleotide-binding leucine-rich repeat (NLR) receptors resulting in localized cell death, thus preventing infection progression (Ali et al., 2018). The hypersensitive immune



response causing cell death is called effector-triggered immunity (ETI), and it causes long-lasting resistance in surrounding tissue (referred to as systemic acquired resistance) (Eves-van den Akker et al., 2021).

Ascarosides are pheromones that coordinate nematode behaviors, dauer development, finding mating partners, social signaling, and even induce host defenses (Ali et al., 2018). Studies have shown that ascarosides signaling and biosynthesis are highly conserved despite nematode diversity, ecology, and phylogeny. Structurally, ascarosides are derivatives of 3,6-dideoxy-L-sugar (ascarylose) and side chains of fatty acids (FA) (Manosalva et al., 2015). Ascarosides are classified based number of carbons in the FA chain. Asc#18 is the most common ascaroside in the *Meloidogyne species* consisting of an 11-carbon FA side chain (Manosalva et al., 2015). A study established that an exogenous application of Asc#18 to *Arabidopsis* roots enhanced its systemic immune resistance against nematodes, bacteria, and fungi (L. Zhao et al., 2016). Upon nematode infection, PRRs perceive conserved nematode-associated molecular patterns (NAMPs) and activate pattern-triggered immunity (PTI) (Manosalva et al., 2015). The evidence of induced basal immune in *Arabidopsis* indicates ascarosides are possible NAMPs (Sato et al., 2019). Two receptors have been associated with the early detection of nematodes, namely, somatic embryogenesis receptor kinase 3 (SERK3), also known as; BRI1-associated receptor kinase 1 (BAK1), and NEMATODE-INDUCED leucine-rich repeat receptor-like kinase receptors (NLR1) (Sato et al., 2019). However, knowledge on the downstream signaling of BAK1 and NLR1 has not been deciphered yet. Notably, the ascaroside receptor elicits PTI in both monocotyledonous and dicotyledonous plants (Vieira & Gleason, 2019). Increasing the expression of ascaroside receptors may provide an opportunity to

generate a heightened ability for the host to identify pathogenic PPN. In addition to ascarosides and nematode effector-proteins, cuticle and chitin are potential candidates for activating NAMPs (Mendy et al., 2017). The cuticle forms the nematode's exoskeleton, vital for its growth and movement, while chitin is the shell that covers the eggshell of PPNs. No molecular patterns for activating NAMPs have been identified yet on the cuticles and chitin.

## **2.9 Co-expression Networks**

Co-expression or co-regulation networks are essential in understanding biological systems, disease pathophysiology and symbiotic or parasitic relationships (Russo et al., 2018). High-dimensional data comprising genomic, proteomic, transcriptomic, metabolomic, and microarray are utilised to construct co-expression networks (Zhang et al., 2014). Advances in high-throughput technologies and reducing costs of large-scale experiments are facilitating the exponential rise in the capture of gene expression profile changes during development, different experimental conditions, environmental and genetic perturbations, treatments, tissues, or cellular levels among others (Serin et al., 2016). The heterogeneous and high-dimensional data richness is not fully extracted while using univariate statistical analysis approaches (Serin et al., 2016). Co-expression analysis tools have multivariate packages or models of handling high dimensional data. Networks can be categorized as associational, mechanistic, or informational (Rhee & Mutwil, 2013). Associational networks are like social interaction networks where genes' characteristics are determined based on their interaction with other genes. Gene properties are extracted from transcriptomic data and utilized to show gene associations resulting in a co-function, co-regulation, or co-expression network. Mechanistic networks (e.g., the lac operon) seek to quantitatively describe and elucidate entire

system functions encoded in an organism's genome. However, it is challenging to uncover the entire breadth and depth of all functions encoded in a genome. Informational networks give details on how functions are linked in a network; for example, the genome-wide metabolic networks and signal transduction networks contain nodes that indicate individual functions. Information networks are sometimes utilized to predict genes responsible for their respective functions.

Association network analysis has shown the intuitive and conceptual potential of investigating, modelling, characterizing and understanding the complex interaction of either specific or whole biological system(s) (Zhang et al., 2014). Association networks provide a representation of the interaction between different biological components. For instance, gene-gene, protein-protein, cell-cell, and transcription factor (TF)-gene interactions are some of the biological system-level domains and functionalities represented by networks (Zhang & Horvath, 2005). Conceptually, association networks are represented by nodes and edges, where nodes represent genes, and edges show the existence of dependency, co-regulation, or correlation relationships among genes (Mason et al., 2009). Association networks have advanced systems biology by investigating complex mechanisms underlying host-microbe interaction, intricate symbiosis, and parasitism. Since root-knot nematodes have a wide range of hosts and developed mechanisms to cope with the immunity of various hosts. The RKN's polyphagous nature and plasticity are anchored in gene expression level, resulting in an advanced host-immunity evasion phenotype. Network analysis of RKN's transcriptomic dataset will aid in understanding the interaction, organization, and function of RKN genes during parasitism. Deciphering biological processes key in

RKN parasitism will help develop mitigation strategies using breeding and crop engineering strategies.

### **2.9.1 Gene Co-expression Network**

Gene expression is the process by which information stored in genes is used to process gene products such as RNA or proteins (Fionda, 2018). The first step of gene expression is transcription, which involves copying gene DNA into RNA (Niu et al., 2019). Gene co-expression networks (GCN) store transcription information occurring at the same condition or time. The GCN analysis facilitates the exploration and clustering of thousands of genes expressed in ranging conditions (Seyfried et al., 2017). The main application of co-expression networks is to find novel genes and assign putative functions to genes under investigation (Wu et al., 2020). However, current co-expression network analysis models have no capacity in providing information on causality, that is, gene activation and inhibition (Bakhtiarizadeh et al., 2020).

Prior to constructing a co-expression network, the sequences data representing different biological conditions is processed from fasta or fastq format into a gene expression matrix (Darzi et al., 2021). The gene expression matrix has rows and columns (of mxn format), where columns (n) contain the number of specific conditions, and each row (m) represents a unique gene (Farhadian et al., 2021). The gene expression matrix contains the count or number of occurrences of each gene in every sample. The weighted gene co-expression network (WGCN) method receives the gene counts to identify co-expression modules (Yin et al., 2019). Filtering the input genes by either variance or mean expression is recommended rather than using differential expression. Usually, filtering by differential expression invalidates the assumption of the scale-free topology.

The filtered gene expression matrix is subsequently subjected to correlation analysis. Correlation between gene pairs is usually quantified by using similarity measures such as Pearson correlation, Spearman's rank correlation, Bi-weight mid correlation, Euclidean distance, and Mutual information to determine co-expression (Chen & Ma, 2021). Each similarity measure has its strengths and limitations. However, Pearson correlation is mainly utilised to generate a quantified similarity matrix that encodes the architecture of the co-expression network (McDonough et al., 2019). The Pearson correlation model detects linear association and connection strength between pair of genes, which take real numbers between -1 and 1, where numbers close to -1 or 1 show strong correlation (Sutherland et al., 2019). The positive real numbers lying between 0 and 1 show a positive correlation meaning that the increase of expression of one gene rises with the increase of the co-expressed gene. Negative numbers (i.e. between -1 and 0) show a negative correlation meaning that the expression of one gene increases with a decrease in the co-expressed gene, and the reverse is true (Langfelder & Horvath, 2008). The similarity matrix containing correlation between gene pairs is transformed into an adjacency matrix through an adjacency function. The adjacency function (is also known as a soft-thresholding function) utilize the similarity matrix to define a weighted correlation network (Oldham et al., 2006). A soft-thresholding principle determines the adjacency function.

The scale-free topology assumption (also known as the power law of distribution) is the critical principle in identifying modules and constructing association networks (Luo et al., 2021). The scale-free topology is intimately associated with the construction and growth of an association network such that a new node preferentially attaches to an already established node. The power-law states that the probability of a node occurring

is inversely proportional to the number of other  $k$  nodes connected to it (Paul et al., 2016). Therefore, the equation defining the occurrence of a node in a network is  $p(k) \sim k^{-\gamma}$ . Thus, scale-free co-expression networks have a high tolerance degree against error or interference (Kan et al., 2021). The nodes' ability to communicate are tolerant even amid disruptions in scale-free networks. For instance, simple organisms persist in growing, reproducing and producing metabolites despite drastic environmental or pharmaceutical interventions (Tan et al., 2013). The ability in which metabolic networks are tolerant against disruptions is attributed to underlying robustness. However, the networks are highly vulnerable to disruptions upon identification, selection, and removal of specific nodes central to network connectivity (Li et al., 2020). GCN construction makes understanding patterns underlying cellular processes possible, which relies on cellular transcriptional responses associated with changing conditions.

The adjacency matrix encodes the connection strength between each pair of nodes. The adjacency matrix can form either an unweighted or a weighted network (Fang et al., 2021). In unweighted networks, the pairwise connection between two nodes is categorized by a binary system of either 1(one) or 0(zero). Where 1 indicates a relationship or connection while 0 indicates no connection between the node pairs (W. Li et al., 2020). In a weighted connection, the pairwise connection between two nodes is expressed by real numbers which range from -1 to 1. Also, the adjacency matrix can either be signed or unsigned. The signed adjacency matrix has positive correlations in  $[0, 1]$  intervals, while the unsigned has negative correlations scaled in  $[-1,0]$  intervals (Seyfried et al., 2017).

As for the removal of spurious correlations, a threshold is selected such that gene pairs that have a correlation score higher than the threshold are considered to have a significant co-expression relationship. The elements in the correlation matrix above the threshold are replaced by 1 (meaning that the corresponding genes are similarly co-expressed), and the remaining elements are replaced by 0.

Lastly, weighted gene co-expression network analysis (WGCNA) has widened the scope of understanding clinical importance, identifying genes of phenotypic significance, screening for candidate biomarkers, understanding transcriptional architecture, annotating genes with regard to module association, comparison of different network topologies, and study meaningful biological associations between co-expression modules, genes products, phenotypes and pathways (Sutherland et al., 2019).

## **2.10 Functional Enrichment of Module Genes**

High-throughput technologies are paving new opportunities for studying the behaviour and relationships of numerous genes and biomolecules (Reimand et al., 2016). Some of the experiments undertaken include establishing mRNA and protein expression levels, the interaction of biomolecules, DNA methylation status, and genotype-phenotype associations. For instance, in gene co-expression network analysis of RNA-seq data, gene clusters of co-regulated genes are established, and interpretation of the clusters is crucial in understanding systems biology (Peterson et al., 2020). Interpretation or enrichment analysis involves associating co-regulated genes to previously curated knowledge of biological processes and pathways to expand knowledge on genome

architecture, gene repertoires, evolution, and molecular mechanisms (Jung et al., 2020). Enrichment analysis is classified into functional or structural annotation achieved through *ab initio* (statistical models) technique or homology-based (sequence similarity) approach. The structural annotation process identifies DNA sequence features such as introns, exons, ESTs, promoters, CDSs, transcription factors (TFs), pseudogenes, etc. (Raudvere et al., 2019). Usually, functional annotation complements structural annotation, where it links biological information to identified biological features or regions. The role of functional analysis is to assess the biochemical, conservation, and variation profiles of the identified features on the molecular and phenotypic levels (Ejigu & Jung, 2020).

Databases are constantly advancing and associating gene identifiers to the numerous knowledge bases is time-consuming. Also, there exists a challenge of getting a consistent consensus and understanding the growing amount of data. The Gene Ontology (GO) Consortium has developed statistical and computational methods to convert noisy data into high-level biological information. Biological process (BP), cellular component (CC), and molecular function (MF) are the main features used by GO to precisely describe millions of genes and their products across many species. Over time, tools have been developed with different approaches of inferring information from GO by using vocabularies, identifiers, or similarity indices. DAVID and Bingo are the most popular tools; however, they have not been updated for years now. The most recently developed enrichment tools are AgriGO (<http://systemsbiology.cau.edu.cn/agriGOv2/>) (Tian et al., 2017), Babelomics (<http://babelomics.bioinfo.cipf.es>) (Medina et al., 2010), Enrichr (<https://maayanlab.cloud/Enrichr>) (Chen et al., 2013), GOstats



(<https://bioconductor.org/packages/release/bioc/html/GOstats.html>) (Falcon & Gentleman, 2007), Metascape (<https://metascape.org>) (Zhou et al., 2019), and g:Profiler tools (<https://biit.cs.ut.ee/gprofiler/gost>) (Reimand et al., 2011).

This study utilised the g:Profiler (version 0.7.0) web-based tool, which is under active and rapid development, easy to use and provides informative visual results. The g:Profiler tool supports diverse gene query identifiers, finding orthologous, and providing a unified functional enrichment report (Reimand et al., 2016). Also, g:Profiler is linked to various databases, therefore, supporting annotation of most species, and it can be utilised via web services, R packages, Java application, or Cytoscape plugins (Kolberg et al., 2018).

## **2.11 Regulatory Motif Finding**

Traditionally, gene expression regulation was considered to occur at the transcription level influenced by activation of transcription factors (Cohen et al., 2014). High expression levels of different mRNA species in an organism do not usually translate to corresponding protein products. Therefore, the amount of protein output is controlled by manipulating mRNA translational ability residing in the untranslated regions (UTRs) (Chatterjee & Pal, 2009). The 5'- and 3'-UTRs are the cis-regulatory elements, and their focal transacting factors alter the stability of the mRNA, its accessibility to the ribosome, its circularisation and interaction with the ribosome (Märtens et al., 2017). The UTR focal points are the poly(A)-binding protein, differential control element (DICE), cytoplasm polyadenylation element (CPE), eukaryotic initiation factor (eIF), and embryonic deadenylation signal (EDEN). RNA transcription activities such as 5' cap structure, endonucleolytic cleavage, RNA editing, and 3' end polyadenylation lead to defining the 5' and 3' UTR regions (Da Rocha et al., 2021).

The 5'-UTRs contain RNA riboswitches and thermometers that regulate mRNA transcription, translation, and stability. Also, RNA-binding proteins bind to the 5'-UTRs by modulating accessibility to ribosome-binding sites on the mRNAs (Ren et al., 2017). The 3' UTR is located between the stop codon and the start of the poly(A) tail, and it contains sequences that influence the fate of mRNA and consequently proteosynthesis (Matoulkova et al., 2012). Nuclear and cytoplasmic polyadenylation are the main processes by which the 3'UTR uses to impact protein synthesis (Mayya & Duchaine, 2019). Nuclear polyadenylation protects the 3'end of the mRNA from degrading endonucleases, facilitates export of the mRNA to the cytoplasm, and ensures the pre-mRNA mature (Preussner et al., 2020). Nuclear polyadenylation involves endonucleolytic cleavage of a pre-mRNA to acquire a poly(A) tail to the 3' end. For a stable and mature mRNA, the 3'end is cleaved at the polyadenylation site (pA site) preferentially after "CA" dinucleotide, and poly(A) polymerase (PAP) facilitates attachment of poly(A) tail comprising from 27 to several thousands of adenines.

Conversely, cytoplasmic polyadenylation regulates mRNA translation of cell cycle controlling genes during early embryogenesis (Bae & Miura, 2020). Usually, mRNAs with shortened poly(A) tails are repressed and stored in the cytoplasm with activation potential. The mRNAs are activated for translation when the poly(A) tails are elongated (Prommana et al., 2013; Yergert et al., 2021). Usually, a mRNA bind to the ribosome, is translated, and finally undergoes deadenylation; thus, the length of the poly(A) tail determines the half-life of an mRNA. No information has yet been established on cis-regulators controlling translation in plant-parasitic nematodes (Britton et al., 2014; Wagner et al., 2013). Growing evidence reveals that translation regulation is as significant as transcript regulation since it is linked to human disease pathophysiology

(Chatterjee & Pal, 2009; Preussner et al., 2020). Through the UTRs, mRNAs for proteins responsible for cell cycles, growth and development, and stress response are regulated at the translation level (Yergert et al., 2021). Defects or mutations at the UTR regions will significantly affect gene expression, associated cellular viability, growth, and development (Bae & Miura, 2020; Gillan et al., 2017). In this study, we sought to establish UTRs responsible for invasive parasite traits such as host selection, host-immunity evasion and establishment of nematode feeding sites.

## CHAPTER THREE

### 3.0 MATERIALS AND METHODS

#### 3.1 Data Acquisition

High-throughput transcription data for various developmental stages of *the M. incognita* were obtained from the Sequence Read Archive (SRA) database at the National Centre for Biotechnology Information (NCBI) under the accession number SRP109232 (Appendix A). The data comprised of five developmental stages including the egg, second juvenile (J2), third juvenile (J3), fourth juvenile (J4), and adult female (Fe). Each stage had three replicates (Choi et al., 2017). The study by Choi et al. (2017) used approximately 1000 eggs of *M. incognita* to infect Nematodes of J2 stage obtained from soil while the J3, J4, and Fe stages were obtained from infected roots and manually identified by microscopy between week 2 and 6 after infection.

#### 3.2 Data Pre-processing

The quality of the raw RNA-seq data was assessed using FastQC software (version 0.11.7) (Leggett et al., 2013). Low-quality reads and adapter sequences were filtered out using Trimmomatic software (version 0.38) using parameters: MILEN: 25, ILLUMINACLIP: Adapters.fa:2:30:20, LEADING: 2, and TRAILING:3 (Bolger et al., 2014). The cleaned reads were re-evaluated for quality using FastQC, and the quality control reports were compiled into one report using MultiQC software (version 1.6) (Ewels et al., 2016).

#### 3.3 Generation of gene-co-regulation matrix

The reference genome of *M. incognita* (under the accession number GCA\_014132215.1\_MINJ2)(<https://ftp.ncbi.nlm.nih.gov/genomes/all/GCA/014/132/>

215/GCA\_014132215.1\_MINJ2/GCA\_014132215.1\_MINJ2\_genomic.fna.gz) was obtained from the Genome database of NCBI to be used for alignment. Filtered reads were aligned against the *M. incognita* reference genome HISAT2 (hierarchical indexing for spliced alignment of transcripts) software (version 2.1.0) (Kim et al., 2015). The reference genome was downloaded from the NCBI genome database and indexed using HISAT2. The indexed referenced genome was formatted to contain genomic features (Kim et al., 2019). Secondly, HISAT2 mapped sample reads were aligned to the indexed reference genome generating sequence alignment/map (SAM) files. Samtools software (version 1.9) was further utilised to sort, index, and convert SAM files into binary alignment/map formatted (BAM) files (Li et al., 2009). Lastly, HTSeq-count python package (version 0.9.1) was utilized to count genome features in the BAM files (Anders et al., 2015). Feature counts of each sample were merged to form a gene expression file in which columns represented samples names, and rows contained gene identifiers. Non-protein coding genes were eliminated from the generation of the gene expression matrix.

### **3.4 Pre-processing of the gene co-expression Matrix**

The R (version 4.0.1) analysis environment was used to filter out genes with low counts from the gene expression matrix using the filterByExpr function of the EdgeR package (version 3.36.0) (Robinson et al., 2009). Normalization of raw counts data was done using log counts per million (log-cpm) and the voom normalization function of the limma package (version 3.48.3) (Smyth et al., 2018). Genes with zero variance and less than 1 cpm in at least three samples were filtered out. The normalisation enabled the expression matrix compatible with the weighted gene co-expression network analysis

(WGCNA) pipeline (which was originally developed to analyse microarray data) (Wu et al., 2020).

### 3.5 Gene co-expression network construction and network visualization

The normalised gene expression matrix of *Meloidogyne incognita* was used to construct a gene-gene co-expression network using the WGCNA package (version 1.69) (Langfelder & Horvath, 2008). The gene co-regulation matrix data was transposed for further analysis such that the columns contained gene identifiers and row names contained sample names (Sutherland et al., 2019). The bi-weight mid correlation was preferred over the Spearman and Pearson correlation to construct a similarity matrix because of its robustness and resistance (Luo et al., 2021). A soft thresholding power ( $\beta$ ) was selected from a scale-free topology fitting index ( $R^2$ ) versus a soft threshold power plot. The soft threshold power was chosen at the saturation point or where the scale-free topology index curve flattens (Kan et al., 2021). The power was utilized to transform the similarity matrix into an adjacency matrix consisting of weights or strength of gene pair connections (Paul et al., 2016). The adjacency matrix was converted into a signed Topological Overlap Matrix (TOM) using the *TOMsimilarity* function, which summarizes connectivity of positively correlated gene pairs (Tan et al., 2013). Using a dissimilarity matrix (1- TOM) as input, the dynamic hybrid tree cutting algorithm identified modules through average linkage hierarchical clustering analysis (Fang et al., 2021). Modules with highly similar expression profiles were merged using the *eigenegeneMerge* function. Lastly, genes with high intra-modular connections were identified as hub genes. The parameters that were used include `corType = "bicor"`, `mergeCutHeight = 0.25`, `minModuleSize = 30`, `networkType = "signed"`, and `TOMType = "signed."` Three files obtained from the WGCNA analysis were important for network

visualization, the edge, node, and node attribute files. The edge file contained gene-gene interaction permutations represented by weights between 0 and 1, (where 0 showed no interaction while 1 signified strong association). The weights were used to represent the connection between nodes. The node file was a representation of all genes present in the network. Finally, the attribute file contained descriptive information of the nodes, their associated module, and the modules colours. The edge, node, and node attribute files obtained from the WGCNA analysis were loaded into Cytoscape (version 3.8.0), and the gene co-expression network and modules were illustrated in different colours (Shannon et al., 2003).

### **3.6 Function Enrichment Analysis**

The "*getBM*" function of the biomaRt package (version 2.50.1) utilised *M.incognita* gene identifiers to query unspliced transcript sequences of module genes from Wormbase (<https://wormbase.org/>) (Smedley et al., 2015). The module gene sequences were saved in multifasta files, which were then parsed into *g:GOSt* function of *g:Profiler* (<https://biit.cs.ut.ee/gprofiler/gost>) web-based tool for functional enrichment (Peterson et al., 2020).

### **3.7 Regulatory Motif Finding and Research Reproducibility**

The "*getBM*" function of the biomaRt package (version 2.50.1) utilised gene identifiers to query unspliced transcript sequences of each module genes from Wormbase (<https://wormbase.org/>) obtaining DNA sequence multifasta file for each module (Howe et al., 2017; Smedley et al., 2015). Using Multiple Expectation maximizations for Motif Elicitation (MEME) (<https://meme-suite.org/meme/tools/meme>) (version 3) (Bailey et al., 2015) suite web tool, highly abundant 3'-UTRs sequences for each

module were determined. The analysis pipelines and codes utilised to generate the gene co-expression network for *M. incognita* are accessible at <https://github.com/NOngeso/Plant-Nematode-Interaction>.



## CHAPTER FOUR

### 4.0 RESULTS

#### 4.1 A weighted gene co-expression network of *Meloidogyne incognita*

A total 30,894 genes were obtained after preprocessing for exploration and for construction of the gene co-expression network.

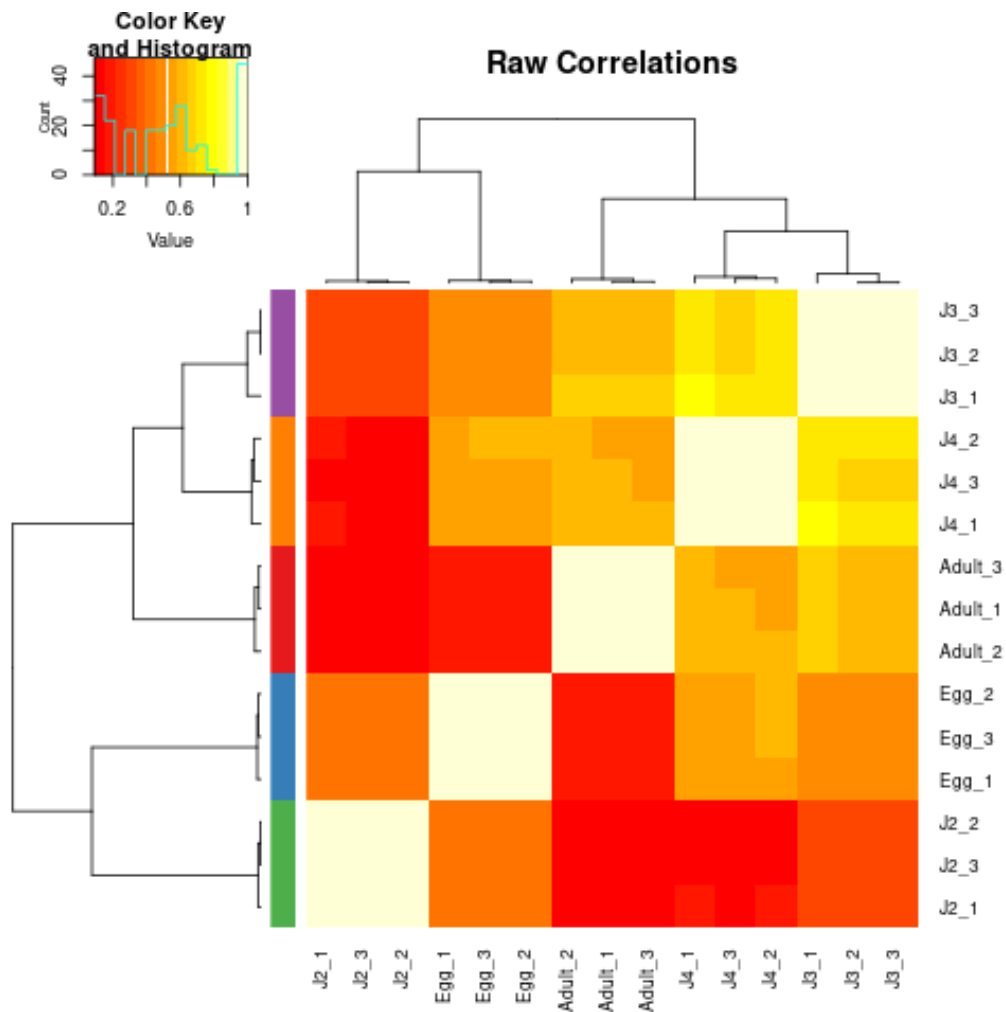


**Figure 4.1:** A hierarchical clustered heat map showing correlation of *M. incognita* gene expression between different developmental stages.

Where Egg = zygote and first vermiform juvenile; J2 = second juvenile; J3 = third sedentary juvenile; J4 = fourth sedentary juvenile; Adult = sedentary female with eggs.

Each sample had three replicates, represented by the underscore and numbers proceeding sample.

The J2, Egg, Adult, J4, and J3 stages are represented by green, blue, red, orange, and green colours respectively on the left side of the correlation heatmap of *M. incognita* (Figure 4.1). The gene correlation between the different developmental stages is as follows J2 and Egg (0.6), J2 and J3 (0.3), J2 and J4, (0.2), J2 and Adult (0.2), J3 and Egg (0.5), J3 and J4 (0.8), J3 and Adult (0.6), J4 and Adult stages (0.8).

## **4.2 Scale-free topology for Adjacency Matrix Construction**

At soft-thresholding power of 16, the power for which the scale-free topology fitting index ( $R^2$ ) was 0.6 (a threshold that achieved a saturation point), was selected (Figure 4.2). The soft-thresholding power was used to convert the similarity matrix into an adjacency matrix containing significantly weighted and correlated.

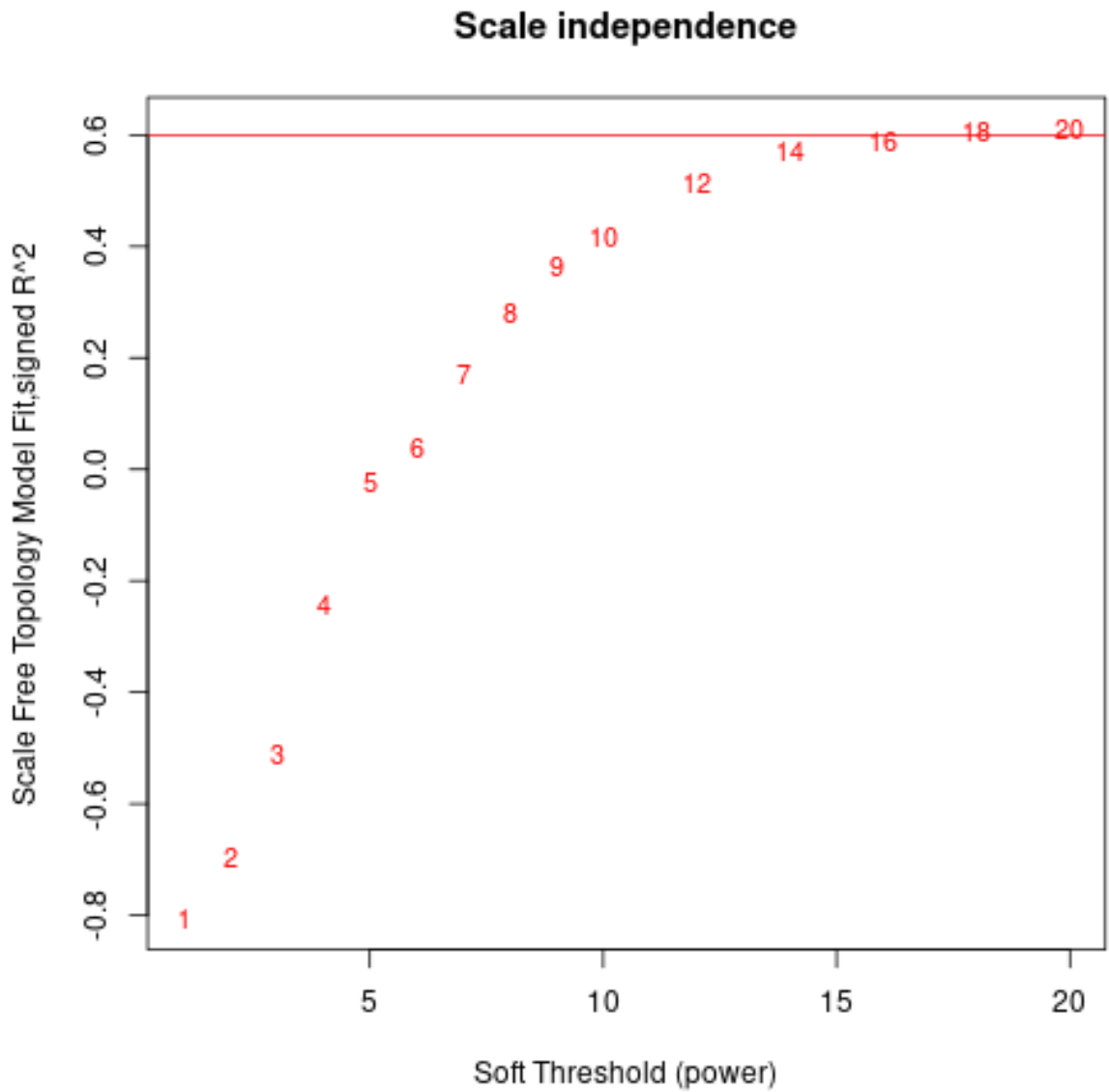


**Figure 4.2:** Illustration of scale free topology of determining adjacency matrix function for constructing *M. incognita's* gene co-expression network.

The red line shows the point at which the  $\beta$  parameter of 16 where soft thresholding was achieved.

### 4.3 Detection of Modules and hub genes in the gene co-expression network of *M. incognita*

A total of 10 meta-modules were generated as illustrated in Figure 4.3 and were used for subsequent analysis of hub gene identification, functional annotation, and determination of abundant regulatory motifs.

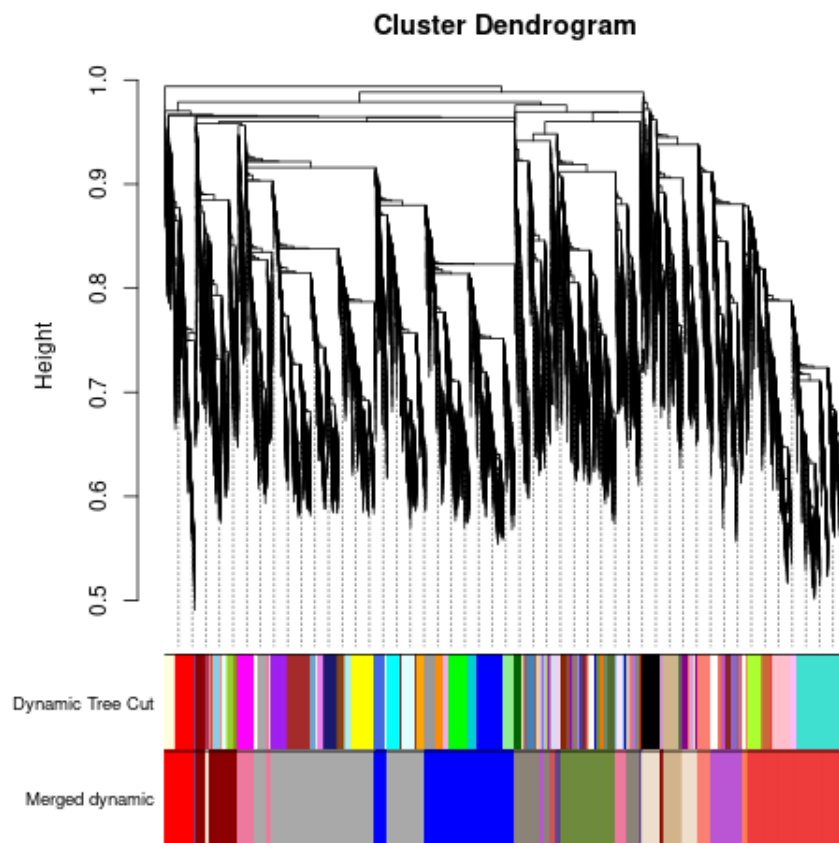


**Figure 4.3:** An illustration of modules in the gene-gene co-expression network of *M. incognita*.

The Dynamic Tree Cut and Merged Dynamic functions present in the WGCNA algorithm were used to identify modules or gene clusters present in the gene co-expression network. Module assignment of genes was depicted in the two-row panels of color on the x-axis, where the upper panel represents a total of 110 identified modules

(Appendix B). In contrast, the lower panel represents ten (10) meta-modules which are clusters of merged modules with similar eigenfactors. The color codes in the panels represent the different modules identified by Dynamic Tree Cut and Merged dynamic analysis functions. The y-axis detects branches in the consensus dendrogram and determines unique gene clusters.

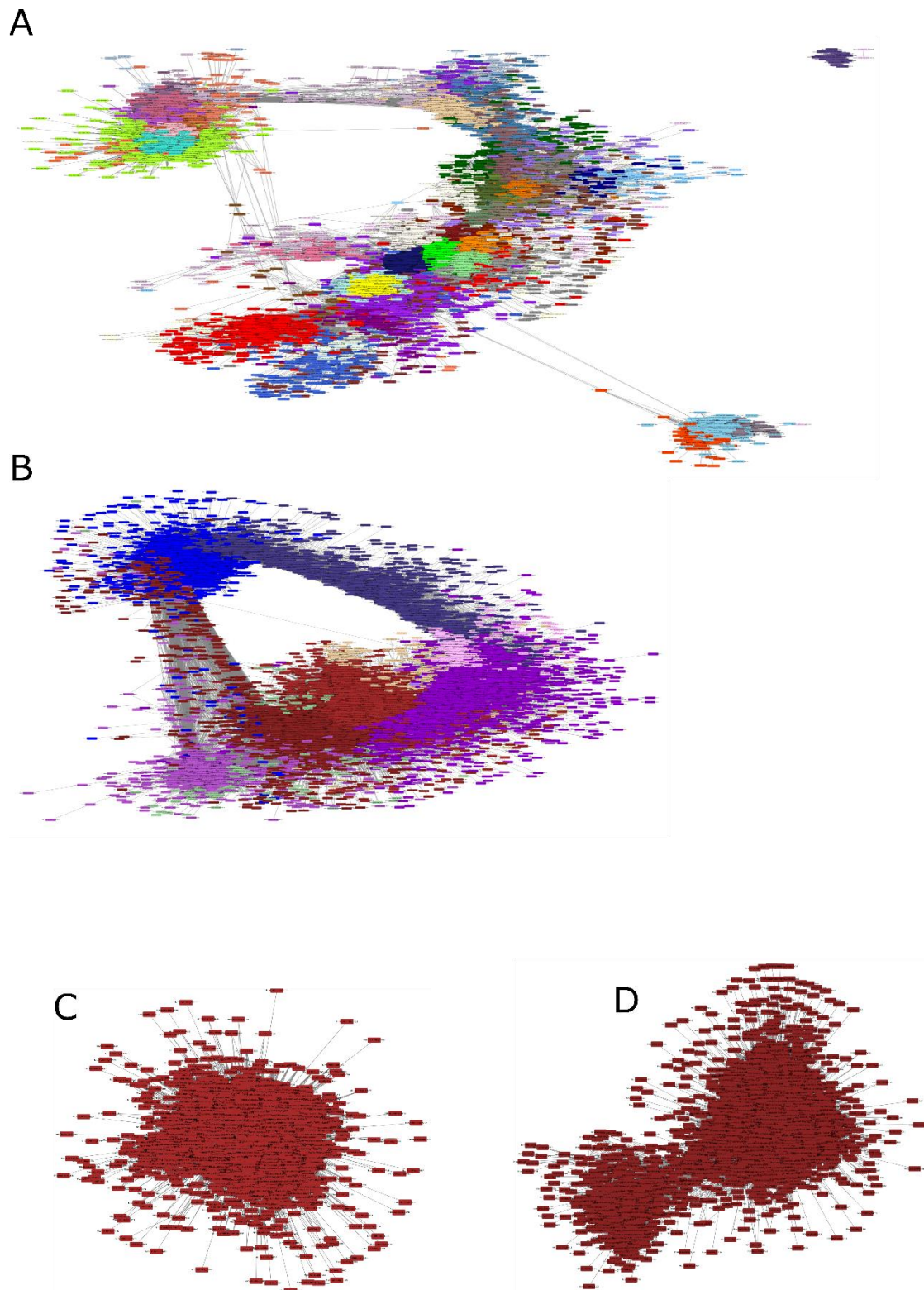


**Figure 4.4(a):** An illustration of the gene co-expression networks and modules of *M. incognita*.

Figure 4.4(a) panel A illustrates a co-expression network containing 30,894 genes resulting in 110 clusters. Panel B illustrates a co-expression network of ten distinct meta-modules resulting from the merging of modules with similar eigengene functions. The co-expression networks show undirected gene to gene interactions where each node represents a gene while edges indicate interaction with a co-expression weight ratio of at least 0.3 between gene pairs. Each meta-module is illustrated using brown4, brown, blue, darkviolet, darkslateblue, mediumorchard, darkseagreen3, plum1, novajowhite2, and mediumpurple1 colours (Figure 4.4(a) and Figure 4.4(b)). The ten meta-modules consist of different gene sizes, as listed in Table 4.1, where the brown module has the most genes (7571), and the mediumpurple1 module has the least number of genes (74).

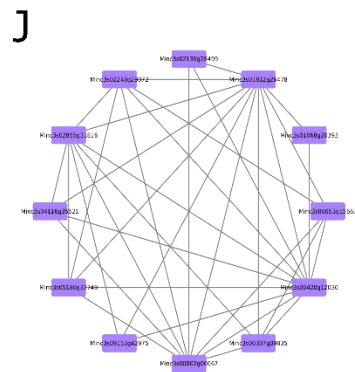
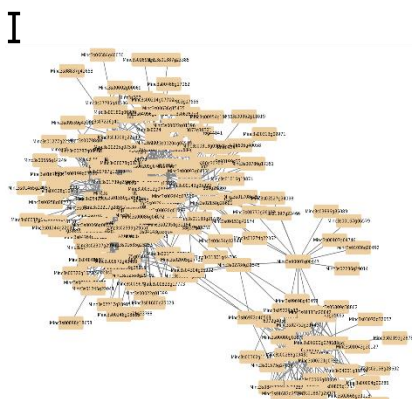
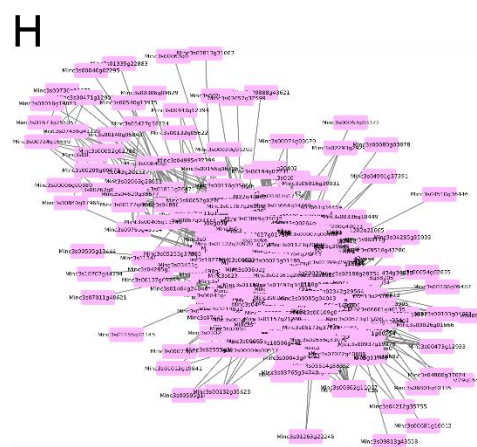
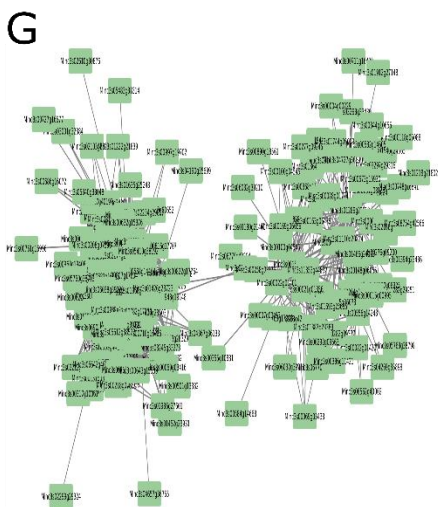
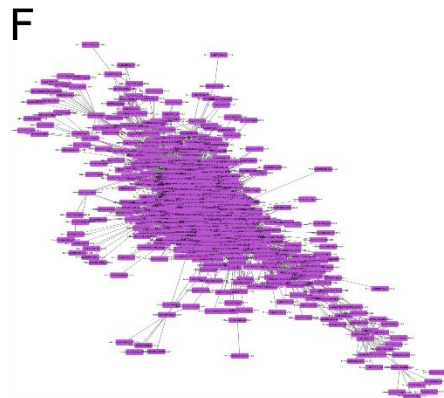
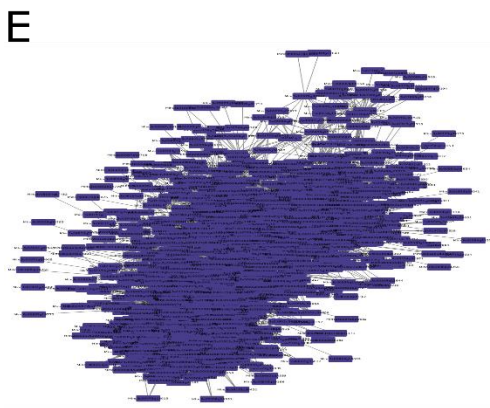
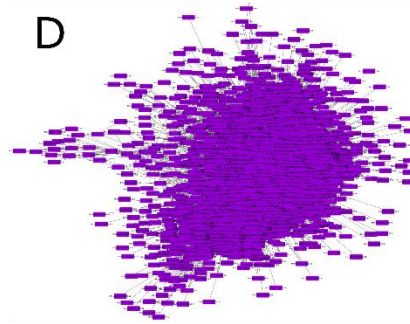
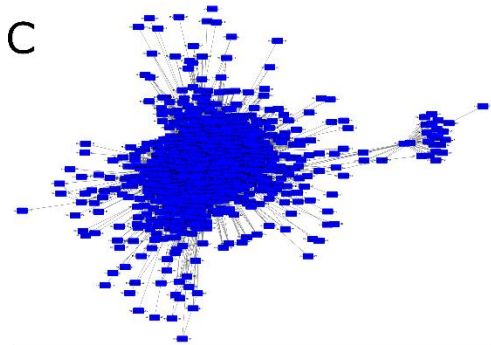




**Figure 4.4(b):** An illustration of ten meta-modules from *M. incognita* merged co-expression network.

Figure 4.4(b) contains panel C, D, E, F, G, H, I, and J which depict the blue, darkviolet, darkslateblue, mediumorchard, darkseagreen3, plum1, novajowhite2, and mediumpurple1 meta-modules respectively. The meta-modules show cluster of genes pair interactions with a weight ratio of ranging between 0.3 to 1.0.

#### **4.4 Functional enrichment of identified Modules and hub genes in the gene-co-expression network of *M. incognita***

##### **4.4.1. Gene set enrichment to determine module molecular function**

Top enriched gene ontology (GO) terms with significant p-value were selected to represent the module's function as listed in Table 4.1.

**Table 4.1:** Summary of the identified modules: hub genes, module size, Top Enriched GO term, and Putative function identified in *Meloidogyne incognita* gene-gene co-expression network using Dynamic Tree Cut clustering method.

Module names	Hub gene ID	Number of genes	Top enriched GO term	GO term adjusted p value
Brown	"Minc3s02273g29200"	7571	Posttranscriptional regulation of gene expression	2.768x10 <sup>-11</sup> (Appendix J)
Brown4	"Minc3s01418g23666"	6217	Peptide biosynthetic process	1.110x10 <sup>-66</sup> (Appendix K)
Blue	"Minc3s01527g24498"	6055	Transmembrane signalling activity	2.481x10 <sup>-104</sup> (Appendix I)
Darkviolet	"Minc3s00284g09370"	4601	Organic substance catabolic process	9.352x10 <sup>-11</sup> (Appendix D)
Darkslateblue	"Minc3s00044g02444"	2250	Transmembrane transport activity	9.875x10 <sup>-25</sup> (Appendix C)
Mediumorchid	"Minc3s03424g33799"	1576	Organonitrogen compound metabolic process	9.054x10 <sup>-9</sup> (Appendix E)
			Glutathione metabolic process	2.679x10 <sup>-6</sup>
Darkseagreen3	"Minc3s01490g24232"	1181	Metallopeptidase activity	2.969x10 <sup>-3</sup> (Appendix L)
Plum1	"Minc3s00035g02069"	788	Transmembrane transport activity	1.129x10 <sup>-15</sup> (Appendix H)
Navajowhite2	"Minc3s00002g00107"	537	Lipid transport	9.761x10 <sup>-1</sup> (Appendix G)
Mediumpurple1	"Minc3s02533g30509"	74	Ras protein signal transduction	7.918x10 <sup>-3</sup> (Appendix F)
			ARF protein signal transduction	1.893x10 <sup>-3</sup>

#### 4.4.2. Gene set enrichment of hub genes.

Hub genes highly interact with most of the genes in a module, making them functionally significant. The hub genes in the 10 modules were determined and their putative biological functions inferred (Table 4.2).

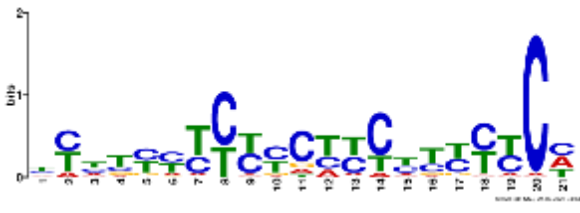
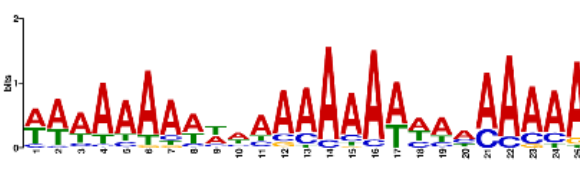
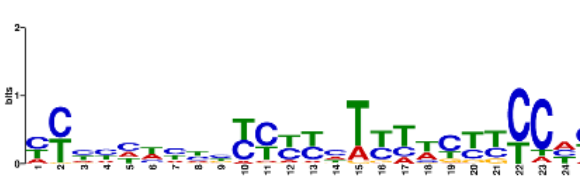
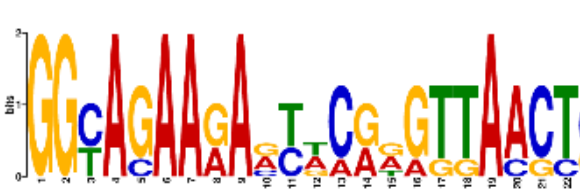
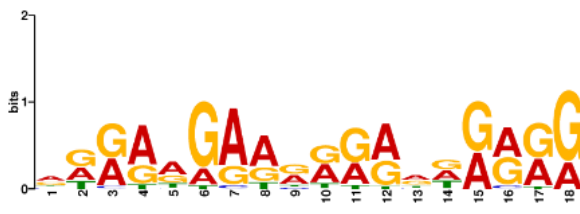
**Table 4.2:** Putative biological functions of module hub genes identified in *Meloidogyne incognita* gene-gene co-expression network using g:Profiler.

Module names	Hub gene ID	Putative biological function
Blue	"Minc3s01527g24498"	regulation of neurotransmitter levels
Brown	"Minc3s02273g29200"	-
Brown4	"Minc3s01418g23666"	chromatin remodeling
Darkseagreen3	"Minc3s01490g24232"	-
Darkslateblue	"Minc3s00044g02444"	nucleoside-diphosphatase activity
Darkviolet	"Minc3s00284g09370"	translational initiation
Mediumorchid	"Minc3s03424g33799"	-
Mediumpurple1	"Minc3s02533g30509"	P-type potassium transmembrane transporter activity
Navajowhite2	"Minc3s00002g00107"	-
Plum1	"Minc3s00035g02069"	-

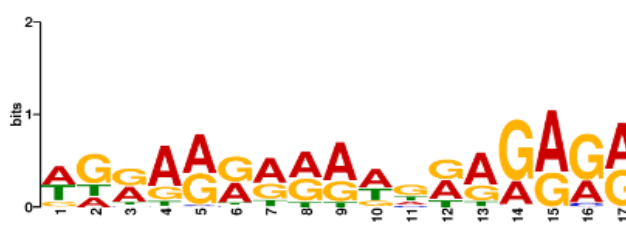
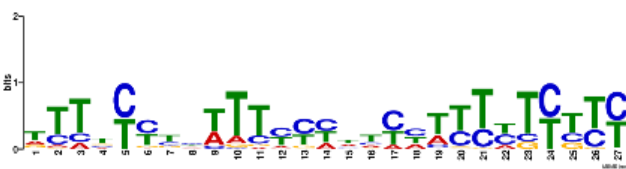
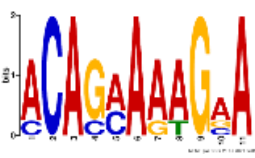
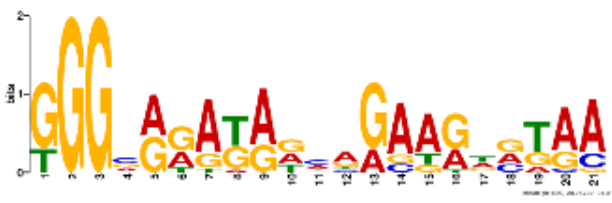
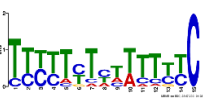
#### **4.5 Identification of 3' untranslated regions (UTR) based on gene co-expression modules**

An abundant regulatory motif expressed for each module was determined using MEME suite web tool (<https://meme-suite.org/meme/>) and illustrated in Table 4.3(a) and Table 4.3(b).

**Table 4.3(a):** Abundantly expressed 3' regulatory motifs in the 10 modules in the Gene Co-expression network of *Meloidogyne incognita* identified using MEME suite web tool.

Module Name	Hub Gene	Regulatory Motif
blue	"Minc3s01527g24 498"	
brown	"Minc3s02273g29 200"	
brown4	"Minc3s01418g23 666"	
darkseagreen3	"Minc3s01490g24 232"	
darkslateblue	"Minc3s00044g02 444"	

**Table 4.3(b):** Abundantly expressed 3' regulatory motifs in the 10 modules in the Gene Co-expression network of *Meloidogyne incognita* identified using MEME suite web tool.

Module Name	Hub Gene	Regulatory Motif
darkviolet	"Minc3s00284g0 9370"	
mediumorc hard	"Minc3s03424g3 3799"	
mediumpur ple1	"Minc3s02533g3 0509"	
navajowhite 2	"Minc3s00002g0 0107"	
plum1	"Minc3s00035g0 2069"	

## CHAPTER FIVE

### 5.0 DISCUSSION

#### 5.1 Construction of a weighted gene co-expression network of *Meloidogyne incognita*

This study uncovered a gene-to-gene interaction network responsible for driving the invasive phenotypic characteristics of *M. incognita*. The gene co-expression network of *M. incognita* was constructed successfully using the power-law distribution principle (also known as the scale-free topology assumption) (Luo et al., 2021). The power-law distribution is intimately associated with the construction and growth of the co-expression network such that nodes are preferentially attached to already established nodes. The scale-free topology tolerates high degree dimensionality of data presented in the gene expression matrix which has 30,194 parameters (genes) for comparison and analysis (Bakhtiarizadeh et al., 2020; Paul et al., 2016). It is postulated that disrupting some of the network's nodes (or genes) will be tolerated since many other supporting genes are in the scale-free network (Luo et al., 2021). For instance, microbes persist in growing, proliferating, and producing metabolites despite drastic environmental or pharmaceutical interventions (Tan et al., 2013).

A total of ten (10) modules formed from clustering of highly interconnected, positively correlated, and co-regulated genes were identified in the gene co-expression network of *M. incognita*. The modules have different gene sizes, and it was presumed that each module has a specific function facilitating the nematode's biological characteristics such as parasitism, growth, development, and metabolism. The brown, brown4, blue, and darkviolet modules are the largest modules having a gene size of 7571, 6217, 6055,

and 4601, respectively. The magnitude of the clusters suggests that the modules facilitate the parasite's behavior in interacting with the host. The study hypothesizes that genes of the same module produce products that foster the cluster's positive coregulation and functional activity. Also, most module genes have sister genes that produce similar metabolomes; thus, the inactivation of one gene does not affect module functioning (Alcalá-Corona et al., 2021; Lecca & Re, 2015).

## **5.2 Functional enrichment of identified Modules and hub genes in the gene-co-expression network of *M. incognita***

The enrichment analysis showed that genes with comparable expression patterns, related activities, and similar end products cluster together implying related roles in the organism's regulatory pathways, physiological processes, metabolism, and parasitic behaviour. The blue, darkslateblue, and plum1 gene co-expression modules were strongly enriched for functional annotation associated with *M. incognita* invasiveness. Minc3s01527g24498, Minc3s00044g02444, and Minc3s00035g02069 represent identifiers of highly connected genes in the three modules. The detection of external and intracellular stimuli to cause changes in *M. incognita* activity is aided by eicosanoid receptors and G-protein coupled receptors (GPCRs). A total of 9093 genes from the three modules are associated with the expression of Nematode Chemosensory GPCRs (NemChRs), and the high gene abundance suggests NemChRs' high diversity of importance in *M. incognita*'s infective juvenile activation, response to host cues, and survival in diverse environments.

Studies have linked NemChRs to host-seeking behaviour witnessed in the infective stage juveniles and free-living nematodes (Langeland et al., 2021). For instance, NemChRs of *Caenorhabditis elegans* is localized at the dendritic cilia of the amphid, a



primary sensory organ nematode (Langeland et al., 2021; Vlaar et al., 2021). The Pigment-dispersing factor (PDF) receptor (PDF-R) and secretin class B GPCR (Seb-3 and Seb-2) are the peptide binding NemChRs that have been found in *C. elegans* (Bernot et al., 2020; Krishnan et al., 2014). Circadian rhythms, reproduction, food regulation, muscle motility/locomotion, energy balance (glucose metabolism), stress response, ethanol tolerance, and neuronal modulation are all regulated by these three receptors (Power et al., 2014; Sengupta et al., 1996). Results obtained in this study suggest that the three modules (blue, darkslateblue, and plum1) enhance the ability of plant parasites to perceive host-derived stimuli, respond to biotic and abiotic signals, and synchronize parasite development with its environment is connected associated with NemChRs (Larsen et al., 2013; Vlaar et al., 2021).

The brown module was found to be enriched for function related to feeding site formation by modulating gene co-expression responsible for inducing the host's growth. It is postulated that the brown module is associated with Glutathione synthase (GS) genes which produce glutathione, a tripeptide molecule composed of glutamate, cysteine, and glycine (Lilley et al., 2018). Glutathione plays an important role in the maintenance of redox homeostasis and cellular defence against oxidative stress. While glutathione itself does not directly alter host transcriptional machinery, it can affect the activity of transcription factors through its interaction with reactive oxygen species (ROS) (Patzewitz et al., 2012). ROS are generated as a by-product of cellular metabolism and can damage DNA, proteins, and lipids. Glutathione helps to neutralize ROS and prevent damage, which can indirectly affect transcriptional activity (Patzewitz et al., 2012). Glutathione also regulates the activity of the transcription factor NF- $\kappa$ B, which plays a key role in immune responses, through the intermediary molecule S-

glutathionylation (Lilley et al., 2018). The 3ODO8 and Hs32EO3 GS genes were identified in *M. incognita* and *Heterodera schachtii*, respectively (Mathers et al., 2017). The GS genes produce mRNA intermediates targeting SCARECROW-like transcription factors in the nuclei of host cells responsible for endoderm differentiation and root radial patterning (Jaouannet & Rosso, 2013; Mejias et al., 2019).

The brown4 module consisting of 6217 genes, forms nematode signalling peptides or effectors that facilitate hijacking the hosts' physiological processes. The hub gene Minc3s01418g23666 and the other module genes are responsible for forming the effector families known to regulate the lifestyle of *M. Incognita*. In *M. incognita*, chorismate mutase (CM) enzymes catalyze the shikimate pathway, resulting in chorismate, a precursor for the formation of auxin, indole-3-acetic acid lignin, and phytoalexins which are essential for root cells differentiation and division (Hassan et al., 2010). Also, CM inhibits the formation of host immune defensive chemicals such as salicylic acid (SA) and flavonoids, thus increasing host plant susceptibility to RKN (Hewezi, 2015).

The darkseagreen3 module was enriched for function associated with peptide bond hydrolysis, which is essential during the development process, invasion of host tissues, and parasite-host interaction. In *C. elegans*, cysteine peptidases (Cathepsins B and L) are involved in embryogenesis, moulting and digestion of nutrients (Curtis, 2007). Peptidases facilitate plant-parasitic nematodes virulence as follows, (1) the proteolytic enzymes digest host tissue proteins to aid parasite penetration and movement until the parasite's establishment site is reached (S. Ali et al., 2015; Craig et al., 2007). (2) Peptidases destroy immunoglobulins linked to nematode surface antigens, thus protecting the parasite against host immune system response (Kovaleva et al., 2004;

Lilley et al., 1999). (3) Peptidases take part in the moulting of PPNs by activating proenzymes to degrade cuticle proteins underlying epidermis (apolysis) and resorbing part of the proteins forming a new one.

The darkviolet and mediumorchard modules were functionally linked to the catabolism of organic substances. Plant-parasitic nematodes withdraw nutrients from the host rich in carbohydrates, lipids, and proteins from the established feeding sites, broken down into amino acids, simple sugars, and fatty acid precursors (Assefa et al., 2021; Mani et al., 2021). Studies have shown that *Caenorhabditis elegans* metabolism pathways are highly conserved, and the precursors formed from the breakdown of macromolecules are required for development, behaviour, and adaptation to environmental changes (Assefa et al., 2021; Watts & Ristow, 2017).

The mediumpurple1 module is responsible for adenosine diphosphate-ribosylation factor (ARF) protein transduction. The ARF family of proteins belongs to the Ras superfamily of small GTPases that play a role in cell differentiation, proliferation, and migration (Dautt-Castro et al., 2021; Wennerberg et al., 2005). In *C. elegans*, the ARF proteins also play a central role in sensory transmission, associative learning, short-term and long-term memory formation (Casalou et al., 2020; Gyurkó et al., 2015). It is postulate that the mediumpurple1 genes of *M. incognita* are therefore associated with olfaction, locomotion, associative learning, and memory formation, which enhance the parasites' ability to be invasive and thwart plant immunity precursors.

Lastly, the navajowhite2 module is involved in lipid transport and metabolism, which is essential during the pre-parasitic second juvenile (ppJ2) phase of the *M. incognita*. During the ppJ2 stage, nematodes have broken loose from the egg and are free in the soil. Since the infective stage has no host yet, it relies predominantly on lipid deposits

on its intestinal and skin-like epidermal cells for energy requirements (Barros et al., 2012; Zhu et al., 2021). Most nematodes have adapted to rely on lipid metabolism because its oxidation generates a great number of ATP molecules as compared to carbohydrates (Branicky et al., 2010; Elle et al., 2008). Neutral lipids such as free cholesterol, monoacylglycerides, diacylglycerides, and cholesterol esters have been characterized in plant-parasitic nematodes (Li et al., 2020; Srinivasan, 2020). The hydrophobic nature of neutral lipids makes them integral structural components in forming cellular and organellar bilayer membranes (Srinivasan, 2015; Watts & Ristow, 2017). Specific lipid composition also influences protein folding and the topology of membranes.

### **5.3 Identification of 3' untranslated regions (UTR) based on gene co-expression modules**

The regulatory motifs were obtained since they are important in establishing mRNA stability and influencing proteosynthesis (Mayya & Duchaine, 2019). Most of the abundant genes present in the different modules of *M. incognita* are not usually transcribed into mRNA and later translated into corresponding protein products since their transcription and translation ability resides in the untranslated regions (UTRs) (Chatterjee & Pal, 2009; Märtens et al., 2017). Thus, these motif features are transaction factors altering mRNA stability, access, and interaction of mRNA to ribosomes (Kozłowski et al., 2021; Märtens et al., 2017). In this study, an abundantly expressed 3'-regulatory motif was determined for each of the ten (10) modules in the gene co-expression network of *M. incognita*. The functions of the established abundant motifs were associated with the enriched functions of module genes as illustrated in (Table 4.3(a) & Table 4.3(b)). The biological significance of 3' untranslated regions provides

insights that potentially link the molecular structure of the nematode with biochemical processes and invasive phenotypic characteristics of the parasite. Targeting the discovered motifs as drug targets will consequently affect the parasite's important physiological processes such as olfactory perception of plant cues that attract the PPN, development cycle, reproduction capability, and expression of effectors facilitating virulence of the parasite. These molecular interfering approaches would enable the protection of the plants against *M. incognita*'s infection (Mangone et al., 2010; Vejnar et al., 2019). Conventional mitigation strategies such as crop rotation, biological controls, and resistant cultivars have limited efficacy against *M. incognita* with a wide host range. Also, the use of inorganic nematicides such as organophosphates, carbamates, and fumigant nematicides pose environmental and human health safety concerns (Bresso et al., 2019).

Regulatory motif targeting presents eco-friendly and potentially effective compounds to mitigate *M. incognita*. The impact of targeting motifs is highly significant compared to targeting specific hub genes or markers (Xia, 2017; Zhang et al., 2016). Organisms have evolved to duplicate the role of essential genes such that it is inconsequential in silencing some of the essential genes (Wu et al., 2016). Therefore, motif targeting drugs will impact the proteosynthesis of essential effectors facilitating the parasite's invasive behavior, metabolism, and physiological positive feedback loops. Regulatory motifs targeting will be specific to *M. incognita*, thus affecting its invasiveness competence. Precision drug targeting will be eco-friendly since no other essential soil microbiomes will be targeted, and it will not negatively alter soil physio-chemical properties.

## CHAPTER SIX

### 6.0 CONCLUSIONS, LIMITATIONS AND RECOMMENDATIONS

#### 6.1 Conclusions

The findings of this study have allowed the following conclusions to be drawn:

- i. A weighted gene co-expression network analysis established key gene associations that are integral in the development of *M. incognita*.
- ii. The hub genes and meta-modules involved in *M. incognita*'s signaling, formation of nematode feeding sites, metabolism, and its growth and development during parasitism were discovered.
- iii. Abundantly expressed 3'-regulatory motifs responsible for mRNA stability and proteosynthesis responsible for physiological functioning and parasitic competence were identified in meta-modules of *M. incognita*.

#### 6.2 Limitations

During the study, these were the discovered the following constraints:

- i. Most functions of *M. incognita* genes and 3'-regulatory motifs were not well documented.

#### 6.3 Recommendations

The following are some of the recommendations made from the current study:

- i. Developing drugs to target the discovered 3'-untranslated regions (UTRs) will consequently affect the physiological functioning and parasitic competence of *M. incognita*.

- ii. Establishing transgenic plants expressing small interfering RNAs (siRNA) targeting the regulatory motifs of *M. incognita*.
- iii. The identified hub genes (Minc3s01527g24498, Minc3s02273g29200, Minc3s01418g23666, Minc3s01490g24232, Minc3s00044g02444, Minc3s00284g09370, Minc3s03424g33799, Minc3s02533g30509, Minc3s00002g00107, and Minc3s00035g02069) are key biomarkers for *M. incognita* that can be used to establish a molecular diagnostic tool.
- iv. Validation studies to determine the potential and efficacy of regulatory motifs as potential targets for nematicide and transgenic plants development are necessary.
- v. It is hypothesized that the motifs found in *M. incognita* are conserved through other plant-parasitic nematodes. Establishing such findings will provide insights into the development of broad-spectrum and eco-friendly toolkits for managing soil parasite burden, thus minimizing crop loss.

## REFERENCES

- Abd-elgawad, M. M. (2021). Optimizing Safe Approaches to Manage Plant-Parasitic Nematodes. *MDPI Plants*, *10*(9), 1911.
- Akinsanya, A. K., Afolami, S. O., Kulakow, P., & Coyne, D. (2020). The root-knot nematode, *Meloidogyne incognita*, profoundly affects the production of popular biofortified cassava cultivars. *Nematology*, *22*(6), 667–676.
- Alcalá-Corona, S. A., Sandoval-Motta, S., Espinal-Enríquez, J., & Hernández-Lemus, E. (2021). Modularity in Biological Networks. *Frontiers in Genetics*, *12*:701331.
- Ali, M., Anjam, M., Nawaz, M., Lam, H., & Chung, G. (2018). Signal transduction in plant–nematode interactions. *International Journal of Molecular Sciences*, *19*(6), 1648.
- Ali, S., Magne, M., Chen, S., Côté, O., Stare, B. G., Obradovic, N., Jamshaid, L., Wang, X., Bélair, G., & Moffett, P. (2015). Analysis of putative apoplastic effectors from the nematode, *Globodera rostochiensis*, and identification of an expansin-like protein that can induce and suppress host defenses. *PLoS ONE*, *10*(1), e0115042.
- Anders, S., Pyl, P. T., & Huber, W. (2015). HTSeq-A Python framework to work with high-throughput sequencing data. *Bioinformatics*, *31*(2), 166–169.
- Assefa, A. D., Kim, S., Mani, V., Ko, H., & Hahn, B. (2021). *Metabolic Analysis of the Development of the Plant-Parasitic Cyst Nematodes Heterodera schachtii and Heterodera trifolii by Capillary Electrophoresis Time-of-Flight Mass Spectrometry*. *22*(19),10488.
- Bae, B., & Miura, P. (2020). Emerging roles for 3' UTRs in neurons. *International*



*Journal of Molecular Sciences*, 21(10), 3413.

Bailey, T. L., Johnson, J., Grant, C. E., & Noble, W. S. (2015). The MEME Suite. *Nucleic Acids Research*, 43(W1), W39–W49.

Bakhtiarizadeh, M. R., Mirzaei, S., Norouzi, M., Sheybani, N., & Vafaei Sadi, M. S. (2020). Identification of Gene Modules and Hub Genes Involved in Mastitis Development Using a Systems Biology Approach. *Frontiers in Genetics*, 11, 722.

Barros, A. G. de A., Liu, J., Lemieux, G. A., Mullaney, B. C., & Ashrafi, K. (2012). Analyses of *C. elegans* Fat Metabolic Pathways. *Methods in Cell Biology*, 107, 383–407.

Bellafiore, S., Shen, Z., Rosso, M. N., Abad, P., Shih, P., & Briggs, S. P. (2008). Direct identification of the *Meloidogyne incognita* secretome reveals proteins with host cell reprogramming potential. *PLoS Pathogens*, 4(10), e1000192.

Bernard, G. C., Egnin, M., & Bonsi, C. (2017). The Impact of Plant-Parasitic Nematodes on Agriculture and Methods of Control. *Nematology-concepts, diagnosis, and control*, 10, 121–151.

Bernot, J. P., Rudy, G., Erickson, P. T., Ratnappan, R., Haile, M., Rosa, B. A., Mitreva, M., O'Halloran, D. M., & Hawdon, J. M. (2020). Transcriptomic analysis of hookworm *Ancylostoma ceylanicum* life cycle stages reveals changes in G-protein coupled receptor diversity associated with the onset of parasitism. *International Journal for Parasitology*, 50(8), 603–610.

Blanc-Mathieu, R., Perfus-Barbeoch, L., Aury, J. M., Da Rocha, M., Gouzy, J., Sallet, E., Martin-Jimenez, C., Bailly-Bechet, M., Castagnone-Sereno, P., Flot, J. F., Kozłowski, D. K., Cazareth, J., Couloux, A., Da Silva, C., Guy, J., Kim-Jo, Y. J.,

- Rancurel, C., Schiex, T., Abad, P., ... Danchin, E. G. J. (2017). Hybridization and polyploidy enable genomic plasticity without sex in the most devastating plant-parasitic nematodes. *PLoS Genetics* 13(6), e1006777.
- Bolger, A. M., Lohse, M., & Usadel, B. (2014). Trimmomatic: A flexible trimmer for Illumina sequence data. *Bioinformatics*, 30(15), 2114–2120.
- Branicky, R., Desjardins, D., Liu, J. L., & Hekimi, S. (2010). Lipid transport and signaling in *Caenorhabditis elegans*. *Developmental Dynamics an official publication of the American Association of Anatomists*, 239(5), 1365–1377.
- Bresso, E., Fernandez, D., Amora, D. X., Noel, P., Petitot, A., Sa, M. L. De, & Albuquerque, E. V. S. (2019). A Chemosensory GPCR as a Potential Target to Control the Root-Knot Nematode *Meloidogyne incognita* Parasitism in Plants. *MDPI Molecules*, 24(20), 3798.
- Britton, C., Winter, A. D., Gillan, V., & Devaney, E. (2014). MicroRNAs of parasitic helminths - Identification, characterization and potential as drug targets. *International Journal for Parasitology: Drugs and Drug Resistance*, 4(2), 85–94.
- Casalou, C., Ferreira, A., & Barral, D. C. (2020). The Role of ARF Family Proteins and Their Regulators and Effectors in Cancer Progression: A Therapeutic Perspective. *Frontiers in Cell and Developmental Biology*, 8(1),217.
- Cetintas, R., Kusek, M., & Fateh, S. A. (2018). Effect of some plant growth-promoting rhizobacteria strains on root-knot nematode , *Meloidogyne incognita* , on tomatoes. *Egyptian Journal of Biological Pest Contro*, 28(1), 1–5.
- Chatterjee, S., & Pal, J. K. (2009). Role of 5'- and 3'-untranslated regions of mRNAs in human diseases. *Biology of the Cell*, 101(5), 251–262.

- Chen, E. Y., Tan, C. M., Kou, Y., Duan, Q., Wang, Z., Meirelles, G. V., Clark, N. R., & Ma'ayan, A. (2013). Enrichr: interactive and collaborative HTML5 gene list enrichment analysis tool. *BMC Bioinformatics*, 14(1), 1-14.
- Chen, X., & Ma, J. (2021). Weighted gene co-expression network analysis (WGCNA) to explore genes responsive to *Streptococcus oralis* biofilm and immune infiltration analysis in human gingival fibroblasts cells. *Bioengineered*, 12(1), 1054–1065.
- Choi, I., Subramanian, P., Shim, D., & Oh, B. (2017). *RNA-Seq of Plant-Parasitic Nematode Meloidogyne incognita at Various Stages of Its Development*. *Frontiers in Genetics* 8(1), 190.
- Cohen, J. E., Lee, P. R., & Fields, R. D. (2014). Systematic identification of 3'-UTR regulatory elements in activity-dependent mRNA stability in hippocampal neurons. *Philosophical Transactions of the Royal Society B: Biological Sciences*, 369(1652), 20130509.
- Cortada, L., Dehennin, I., Bert, W., & Coyne, D. (2019). Integration of nematology as a training and research discipline in sub-Saharan Africa: progress and prospects. *Nematology*, 22(1), 1–21.
- Cox, D., Reilly, B., Warnock, N. D., Dyer, S., Sturrock, M., Cortada, L., Coyne, D., Maule, A. G., & Dalzell, J. J. (2019a). Transcriptional signatures of invasiveness in *Meloidogyne incognita* populations from sub-Saharan Africa. *International Journal for Parasitology*, 49(11), 837–841.
- Cox, D., Reilly, B., Warnock, N. D., Dyer, S., Sturrock, M., Cortada, L., Coyne, D., Maule, A. G., & Dalzell, J. J. (2019b). Transcriptional signatures of invasiveness

- in *Meloidogyne incognita* populations from sub-Saharan Africa. *International Journal for Parasitology*, *49*(11), 837–841.
- Coyne, D. L., Cortada, L., Dalzell, J. J., Claudius-Cole, A. O., Haukeland, S., Luambano, N., & Talwana, H. (2018). Plant-parasitic nematodes and food security in Sub-Saharan Africa. *Annual Review of Phytopathology*, *56*, 381–403.
- Coyne, D. L., Omowumi, A., Rotifa, I., & Afolami, S. O. (2013). Pathogenicity and damage potential of five species of plant-parasitic nematodes on plantain (*Musa* spp., AAB genome) cv. Agbagba. *Nematology*, *15*(5), 589–599.
- Craig, H., Isaac, R. E., & Brooks, D. R. (2007). Unravelling the moulting degradome : new opportunities for chemotherapy ? *Trends in Parasitology*, *23*(6), 248-253.
- Curtis, R. H. C. (2007). Plant parasitic nematode proteins and the host parasite interaction. *Oxford University Press*, *6*(1), 50–58.
- Da Rocha, M., Bournaud, C., Dazenière, J., Thorpe, P., Bailly-Bechet, M., Pellegrin, C., Péré, A., Grynberg, P., Perfus-Barbeoch, L., Eves-van den Akker, S., & Danchin, E. G. J. (2021). Genome Expression Dynamics Reveal the Parasitism Regulatory Landscape of the Root-Knot Nematode *Meloidogyne incognita* and a Promoter Motif Associated with Effector Genes. *Genes*, *12*(5), 771.
- Dahlin, P., Eder, R., Consoli, E., Krauss, J., & Kiewnick, S. (2019). Integrated control of *Meloidogyne incognita* in tomatoes using fluopyram and *Purpureocillium lilacinum* strain 251. *Crop Protection*, *124*, 104874.
- Darzi, M., Gorgin, S., Majidzadeh-A, K., & Esmaili, R. (2021). Gene co-expression network analysis reveals immune cell infiltration as a favorable prognostic marker in non-uterine leiomyosarcoma. *Scientific Reports*, *11*(1), 1–11.

- Dautt-Castro, M., Rosendo-Vargas, M., & Casas-Flores, S. (2021). The small gtpases in fungal signaling conservation and function. *Cells*, *10*(5), 1039.
- De Medeiros, H. A., De Araújo Filho, J. V., De Freitas, L. G., Castillo, P., Rubio, M. B., Hermosa, R., & Monte, E. (2017). Tomato progeny inherit resistance to the nematode *Meloidogyne javanica* linked to plant growth induced by the biocontrol fungus *Trichoderma atroviride*. *Scientific Reports*, *7*(1), 1–13.
- Dubreuil, G., Magliano, M., Deleury, E., Abad, P., & Rosso, M. N. (2007). Transcriptome analysis of root-knot nematode functions induced in the early stages of parasitism. *New Phytologist* *176*(2), 426–436.
- Ejigu, G. F., & Jung, J. (2020). Review on the computational genome annotation of sequences obtained by next-generation sequencing. *Biology*, *9*(9), 295.
- El-Sappah, A. H., Islam, M. M., El-Awady, H. H., Yan, S., Qi, S., Liu, J., Cheng, G. T., & Liang, Y. (2019). Tomato natural resistance genes in controlling the root-knot nematode. *Genes*, *10*: 925.
- Elle, I. C., Olsen, L. C. B., Mosbech, M. B., Rødkær, S. V., Pultz, D., Boelt, S. G., Fredens, J., Sørensen, P., & Færgeman, N. J. (2008). *C. Elegans*: A model for understanding lipid accumulation. *Lipid Insights*, *1*, LPI-S1057.
- Eves-van den Akker, S., Stojilković, B., & Gheysen, G. (2021). Recent applications of biotechnological approaches to elucidate the biology of plant–nematode interactions. *Current Opinion in Biotechnology*, *70*, 122–130.
- Ewels, P., Magnusson, M., Lundin, S., & Käller, M. (2016). MultiQC: Summarize analysis results for multiple tools and samples in a single report. *Bioinformatics*, *32*(19), 3047–3048.

- Falcon, S., & Gentleman, R. (2007). Using GOSTATS to test gene lists for GO term association. *Bioinformatics*, *23*(2), 257–258.
- Fang, Q., Wang, Q., Zhou, Z., & Xie, A. (2021). Consensus analysis via weighted gene co-expression network analysis (WGCNA) reveals genes participating in early phase of acute respiratory distress syndrome (ARDS) induced by sepsis. *Bioengineered*, *12*(1), 1161–1172.
- Farhadian, M., Rafat, S. A., Panahi, B., & Mayack, C. (2021). Weighted gene co-expression network analysis identifies modules and functionally enriched pathways in the lactation process. *Scientific Reports*, *11*(1), 1–15.
- Ferris, H., Griffiths, B. S., Porazinska, D. L., Powers, T. O., Wang, K. H., & Tenuta, M. (2012). Reflections on plant and soil nematode ecology: Past, present and future. *Journal of Nematology*, *44*(2), 115–126.
- Fionda, V. (2018). Networks in biology. *Encyclopedia of Bioinformatics and Computational Biology: ABC of Bioinformatics*, *13*, 915–921.
- Fitoussi, N., Borrego, E., Kolomiets, M. V., Qing, X., Bucki, P., Sela, N., Belausov, E., & Braun Miyara, S. (2021). Oxylipins are implicated as communication signals in tomato–root-knot nematode (*Meloidogyne javanica*) interaction. *Scientific Reports*, *11*(1), 1–16.
- Gheysen, G., & Fenoll, C. (2002). Gene expression in nematode feeding sites. *Annual Review of Phytopathology*, *40*(1), 191–219.
- Gillan, V., Maitland, K., Laing, R., Gu, H., Marks, N. D., Winter, A. D., Bartley, D., Morrison, A., Skuce, P. J., Rezansoff, A. M., Gilleard, J. S., Martinelli, A., Britton, C., & Devaney, E. (2017). Increased expression of a microRNA correlates with

- anthelmintic resistance in parasitic nematodes. *Frontiers in Cellular and Infection Microbiology*, 7,452.
- Goyena, R. (2019). Development of the Root-Knot Nematode Feeding Cell. In *Journal of Chemical Information and Modeling* 53(9).
- Grunewald, W., Cannoot, B., Friml, J., & Gheysen, G. (2009). Parasitic nematodes modulate PIN-mediated auxin transport to facilitate infection. *PLoS Pathogens*, 5(1), e1000266.
- Gyurkó, M. D., Csermely, P., Soti, C., & Steták, A. (2015). Distinct roles of the RasGAP family proteins in *C. elegans* associative learning and memory. *Scientific Reports*, 5(1), 1–10.
- Hassan, S., Behm, C. A., & Mathesius, U. (2010). Effectors of plant parasitic nematodes that re-program root cell development. *Functional Plant Biology*, 37(10), 933–942.
- Hewezi, T. (2015). Cellular signaling pathways and posttranslational modifications mediated by nematode effector proteins. *Plant Physiology*, 169(2), 1018–1026.
- Howe, K. L., Bolt, B. J., Shafie, M., Kersey, P., & Berriman, M. (2017). WormBase ParaSite – a comprehensive resource for helminth genomics. *Molecular and Biochemical Parasitology*, 215, 2–10.
- Hu, H., Gao, Y., Li, X., Chen, S., Yan, S., & Tian, X. (2020). Identification and nematicidal characterization of proteases secreted by endophytic bacteria *Bacillus cereus* BCM2. *Phytopathology*, 110(2), 336–344.
- Iberkleid, I., Vieira, P., de Almeida Engler, J., Firester, K., Spiegel, Y., & Horowitz, S.

- B. (2013). Fatty Acid-and Retinol-Binding Protein, Mj-FAR-1 Induces Tomato Host Susceptibility to Root-Knot Nematodes. *PLoS ONE*, 8(5), 1–14.
- Id, X. W., Yu, H., Yang, R., Zhou, Y., Zhu, X., Wang, Y., Liu, X., Fan, H., Chen, L., & Duan, Y. (2019). Evaluation of suitable reference genes for gene expression analysis in the northern root- knot nematode , *Meloidogyne hapla*. *PLoS one*, 15(1), 1–15.
- Isagie, M. V, Ienie, C. M. S. M., Arais, M. M., Aneel, M. D., Arssen, G. K., & Ourie, H. F. (2018). *Short communication Identification of Meloidogyne spp . associated with agri- and horticultural crops in South Africa*. 20(4), 397–401.
- Jaouannet, M., & Rosso, M. N. (2013). Effectors of root sedentary nematodes target diverse plant cell compartments to manipulate plant functions and promote infection. *Plant Signaling and Behavior*, 8(9), e25507.
- Jaubert, S., Milac, A. L., Petrescu, A. J., De Almeida-Engler, J., Abad, P., & Rosso, M. N. (2005). In planta secretion of a calreticulin by migratory and sedentary stages of root-knot nematode. *Molecular Plant-Microbe Interactions*, 18(12), 1277–1284.
- Jones, J. T., Haegeman, A., Danchin, E. G. J., Gaur, H. S., Helder, J., Jones, M. G. K., Kikuchi, T., Manzanilla-López, R., Palomares-Rius, J. E., Wesemael, W. M. L., & Perry, R. N. (2013). Top 10 plant-parasitic nematodes in molecular plant pathology. *Molecular Plant Pathology*, 14(9), 946–961.
- Jung, H., Ventura, T., Sook Chung, J., Kim, W. J., Nam, B. H., Kong, H. J., Kim, Y. O., Jeon, M. S., & Eyun, S. Il. (2020). Twelve quick steps for genome assembly and annotation in the classroom. *PLoS Computational Biology*, 16(11), e1008325.



- Kaloshian, I., & Teixeira, M. (2019). Advances in Plant-Nematode Interactions with Emphasis on the Notorious Nematode Genus *Meloidogyne*. *Phytopathology*, 109(12), 1988-1996.
- Kan, K. J., Guo, F., Zhu, L., Pallavi, P., Sigl, M., & Keese, M. (2021). Weighted gene co-expression network analysis reveals key genes and potential drugs in abdominal aortic aneurysm. *Biomedicines*, 9(5), 546.
- Kanfra, X., Liu, B., Beerhues, L., Sørensen, S. J., & Heuer, H. (2018). Free-living nematodes together with associated microbes play an essential role in apple replant disease. *Frontiers in Plant Science*, 9(1), 1666.
- Karuri, H. W., Olago, D., Neilson, R., Njeri, E., Opere, A., & Ndegwa, P. (2017). Plant parasitic nematode assemblages associated with sweet potato in Kenya and their relationship with environmental variables. *Tropical Plant Pathology*, 42(1), 1–12.
- Kim, D., Langmead, B., & Salzberg, S. L. (2015). HISAT: a fast spliced aligner with low memory requirements Daehwan HHS Public Access. *Nature Methods*, 12(4), 357–360.
- Kim, D., Paggi, J. M., Park, C., Bennett, C., & Salzberg, S. L. (2019). Graph-based genome alignment and genotyping with HISAT2 and HISAT-genotype. *Nature Biotechnology*, 37(8), 907–915.
- Kiyohara, S., & Sawa, S. (2012). CLE signaling systems during plant development and nematode infection. *Plant and Cell Physiology*, 53(12), 1989–1999.
- Kolberg, L., Kuzmin, I., Adler, P., Vilo, J., & Peterson, H. (2018). FuncExplorer: A tool for fast data-driven functional characterisation of high-throughput expression data. *BMC Genomics*, 19(1), 1–17.

- Kovaleva, E. S., Masler, E. P., Skantar, A. M., & Chitwood, D. J. (2004). Novel matrix metalloproteinase from the cyst nematodes *Heterodera glycines* and *Globodera rostochiensis*. *Molecular and Biochemistry Parasitology*, *136*, 109–112.
- Kozłowski, D. K. L., Hassanaly-Goulamhousen, R., Da Rocha, M., Koutsovoulos, G. D., Bailly-Bechet, M., & Danchin, E. G. J. (2021). Movements of transposable elements contribute to the genomic plasticity and species diversification in an asexually reproducing nematode pest. *Evolutionary Applications*, *14*(7), 1844–1866.
- Krishnan, A., Almén, M. S., Fredriksson, R., & Schiöth, H. B. (2014). Insights into the origin of nematode chemosensory GPCRs: Putative orthologs of the *srw* family are found across several phyla of protostomes. *PLoS ONE*, *9*(3), 1–12.
- Kumar, P., Id, S. K., Silva, M. Da, Singh, R., Davis, R. F., Nichols, R. L., & Id, P. W. C. (2019). *Transcriptome analysis of a nematode resistant and susceptible upland cotton line at two critical stages of Meloidogyne incognita infection and development*. *14*(9), 1–19.
- Langat, J. ., J.W., K., Muiru, W. M., & Otieno, W. (2008). Response of Free-Living Nematodes to Treatments Targeting Plant Parasitic Nematodes in Carnation. *Asian Journal of Plant Sciences*, *7*(5), 467–472.
- Langeland, A., Hawdon, J. M., & Halloran, D. M. O. (2021). NemChR-DB : a database of parasitic nematode chemosensory G-protein coupled receptors. *International Journal for Parasitology*, *51*(5), 333–337.
- Langfelder, P., & Horvath, S. (2008). WGCNA: An R package for weighted correlation network analysis. *BMC Bioinformatics*, *9*(1), 1–13.

- Larsen, M. J., Ruiz, E., Williams, T., Lowery, D. E., Geary, T. G., & Kubiak, T. M. (2013). International Journal for Parasitology: Drugs and Drug Resistance Functional expression and characterization of the *C. elegans* G-protein-coupled FLP-2 Receptor ( T19F4 . 1 ) in mammalian cells and yeast. *International Journal for Parasitology: Drugs and Drug Resistance*, 3, 1–7.
- Lecca, P., & Re, A. (2015). Detecting modules in biological networks by edge weight clustering and entropy significance. *Frontiers in Genetics*, 6(1), 265.
- Leggett, R. M., Ramirez-Gonzalez, R. H., Clavijo, B. J., Waite, D., & Davey, R. P. (2013). Sequencing quality assessment tools to enable data-driven informatics for high throughput genomics. *Frontiers in Genetics*, 4(1), 288.
- Li, H., Handsaker, B., Wysoker, A., Fennell, T., Ruan, J., Homer, N., Marth, G., Abecasis, G., & Durbin, R. (2009). The Sequence Alignment/Map format and SAMtools. *Bioinformatics*, 25(16), 2078–2079.
- Li, W., Wang, L., Wu, Y., Yuan, Z., & Zhou, J. (2020). Weighted gene co-expression network analysis to identify key modules and hub genes associated with atrial fibrillation. *International Journal of Molecular Medicine*, 45(2), 401–416.
- Li, Y., Ding, W., Li, C. Y., & Liu, Y. (2020). HLH-11 modulates lipid metabolism in response to nutrient availability. *Nature Communications*, 11(1), 1–13.
- Lilley, C. J., Devlin, P., Urwin, P. E., Atkinson, H. J., Lilley, C., Devlin, P., Urwin, P., & Atkinson, H. (1999). Parasitic Nematodes, Proteinases and Transgenic Plants. *Parasitology Today*, 15(10), 414-417.
- Lilley, C. J., Maqbool, A., Wu, D., Yusup, H. B., Jones, L. M., Birch, P. R. J., Banfield, M. J., Urwin, P. E., & Akker, S. E. Den. (2018). Effector gene birth in plant

- parasitic nematodes: Neofunctionalization of a housekeeping glutathione synthetase gene. *PLoS Genetics*, *14*(4), 1–26.
- Lin, B., Zhuo, K., Chen, S., Hu, L., Sun, L., Wang, X., Zhang, L., & Liao, J. (2016). A novel nematode effector suppresses plant immunity by activating host reactive oxygen species-scavenging system. *New Phytologist*, *209*(3), 1159–1173.
- Luo, X., Feng, L., Xu, W. B., Bai, X. J., & Wu, M. N. (2021). Weighted gene co-expression network analysis of hub genes in lung adenocarcinoma. *Evolutionary Bioinformatics*, *17*(1), 117693343211009898.
- Lynn, O. M., Song, W. G., Shim, J. K., Kim, J. E., & Lee, K. Y. (2010). Effects of azadirachtin and neem-based formulations for the control of sweetpotato whitefly and root-knot nematode. *Journal of Applied Biological Chemistry*, *53*(5), 598–604.
- Majdi, N., & Traunspurger, W. (2015). Free-living nematodes in the freshwater food web: A review. *Journal of Nematology*, *47*(1), 28–44.
- Mangone, M., Manoharan, A. P., Thierry-Mieg, D., Thierry-Mieg, J., Han, T., Mackowiak, S. D., Mis, E., Zegar, C., Gutwein, M. R., Khivansara, V., Attie, O., Chen, K., Salehi-Ashtiani, K., Vidal, M., Harkins, T. T., Bouffard, P., Suzuki, Y., Sugano, S., Kohara, Y., ... Kim, J. K. (2010). The landscape of *C. elegans* 3'UTRs. *Science*, *329*(5990), 432–435.
- Mani, V., Assefa, A. D., & Hahn, B. S. (2021). Transcriptome analysis and mirna target profiling at various stages of root-knot nematode *Meloidogyne incognita* development for identification of potential regulatory networks. *International Journal of Molecular Sciences*, *22*(14), 1–20.

- Manosalva, P., Manohar, M., Reuss, S. H. Von, Chen, S., Koch, A., Kaplan, F., Choe, A., Micikas, R. J., Wang, X., Kogel, K., Sternberg, P. W., Williamson, V. M., Schroeder, F. C., & Klessig, D. F. (2015). plant defenses and pathogen resistance. *Nature Communications*, 6(1), 7795.
- Märtens, B., Sharma, K., Urlaub, H., & Bläsi, U. (2017). The SmAP2 RNA binding motif in the 3'UTR affects mRNA stability in the crenarchaeum *Sulfolobus solfataricus*. *Nucleic Acids Research*, 45(15), 8957–8967.
- Marteu, N., Magnone, V., Lebrigand, K., Cabrera, J., Barcala, M., Cl, A., Millar, A., Escobar, C., Abad, P., & Favery, B. (2017). Characterization of microRNAs from *Arabidopsis* galls highlights a role for miR159 in the plant response to the root-knot nematode *Meloidogyne incognita* Cl. *New Phytologist*, 216(1), 882–896.
- Mason, M. J., Fan, G., Plath, K., Zhou, Q., & Horvath, S. (2009). Signed weighted gene co-expression network analysis of transcriptional regulation in murine embryonic stem cells. *BMC Genomics*, 10(1), 1–10.
- Mathers, T. C., Chen, Y., Kaithakottil, G., Legeai, F., Mugford, S. T., Baa-puyoulet, P., Bretaudeau, A., Clavijo, B., Colella, S., Collin, O., Dalmay, T., Derrien, T., Feng, H., Gabaldón, T., Jordan, A., Julca, I., Kettles, G. J., Kowitzanich, K., Lavenier, D., ... Wilson, A. C. C. (2017). Rapid transcriptional plasticity of duplicated gene clusters enables a clonally reproducing aphid to colonise diverse plant species. *Genome Biology*, 27(1), 1–20.
- Mathew, R., & Opperman, C. H. (2020). Current insights into migratory endoparasitism: Deciphering the biology, parasitism mechanisms, and management strategies of key migratory endoparasitic phytonematodes. *Plants*,

9(6), 1–17.

Matoulkova, E., Michalova, E., Vojtesek, B., & Hrstka, R. (2012). The role of the 3' untranslated region in post-transcriptional regulation of protein expression in mammalian cells. *RNA Biology*, 9(5), 563–576.

Mayya, V. K., & Duchaine, T. F. (2019). Ciphers and executioners: How 3' untranslated regions determine the fate of messenger RNAs. *Frontiers in Genetics*, 10(1), 1–18.

Mccarter, J. P., Mitreva, M. D., Martin, J., Wylie, T., Rao, U., Pape, D., Bowers, Y., Murphy, C. V, Kloek, A. P., Chiapelli, B. J., Clifton, W., Bird, D. M., & Waterston, R. H. (2003). Analysis and functional classification of transcripts from the nematode *Meloidogyne incognita*. *Genome biology*, 4, 1–19.

McDonough, J. E., Kaminski, N., Thienpont, B., Hogg, J. C., Vanaudenaerde, B. M., & Wuyts, W. A. (2019). Gene correlation network analysis to identify regulatory factors in idiopathic pulmonary fibrosis. *Thorax*, 74(2), 132–140.

Medina, C., Rocha, M., Magliano, M., Raptopoulo, A., Marteu, N., Lebrigand, K., Abad, P., Favery, B., & Jaubert-possamai, S. (2018). Characterization of siRNAs clusters in *Arabidopsis thaliana* galls induced by the root-knot nematode *Meloidogyne incognita*. *BMC Genomics*, 19(943), 1–16.

Medina, I., Carbonell, J., Pulido, L., Madeira, S. C., Goetz, S., Conesa, A., Tárraga, J., Pascual-Montano, A., Nogales-Cadenas, R., Santoyo, J., García, F., Marbà, M., Montaner, D., & Dopazo, J. (2010). Babelomics: An integrative platform for the analysis of transcriptomics, proteomics and genomic data with advanced functional profiling. *Nucleic Acids Research*, 38(2), W210–W213.

- Mejias, J., Truong, N. M., Abad, P., Favery, B., & Quentin, M. (2019). Plant Proteins and Processes Targeted by Parasitic Nematode Effectors. *Frontiers in Plant Science*, *10*(1), 1–10.
- Melillo, M. T., Leonetti, P., Bongiovanni, M., Castagnone-Sereno, P., & Bleve-Zacheo, T. (2006). Modulation of reactive oxygen species activities and H<sub>2</sub>O<sub>2</sub> accumulation during compatible and incompatible tomato-root-knot nematode interactions. *New Phytologist*, *170*(3), 501–512.
- Mendy, B., Wanjiku, M., Radakovic, Z. S., Holbein, J., Ilyas, M., Chopra, D., Holton, N., Zipfel, C., Grundler, F. M. W., & Siddique, S. (2017). Arabidopsis leucine-rich repeat receptor – like kinase NILR1 is required for induction of innate immunity to parasitic nematodes. *PLoS Pathogens*, *13*(4), 1–22.
- Moens, M. (2009). Meloidogyne Species – a Diverse Group of Novel and Important Plant Parasites. *CAB International*, *1*(1), 1–17.
- Molinari, S., & Miacola, C. (1997). Antioxidant Enzymes in Phytoparasitic Nematodes. *Journal of Nematology*, *29*(2), 153–159.
- Monokrousos, N., Argyropoulou, M. D., Tzani, K., Menkissoglou-Spiroudi, U., Boutsis, G., D’Addabbo, T., & Ntalli, N. (2021). The effect of botanicals with nematicidal activity on the structural and functional characteristics of the soil nematode community. *MDPI Agriculture*, *11*(4), 1–12.
- Niu, X., Zhang, J., Zhang, L., Hou, Y., Pu, S., Chu, A., Bai, M., & Zhang, Z. (2019). Weighted Gene Co-Expression Network Analysis Identifies Critical Genes in the Development of Heart Failure After Acute Myocardial Infarction. *Frontiers in Genetics*, *10*(November), 1–17.

- Ntidi, K. N., Daneel, M. S., & Fourie, H. (2019). The host status of *Amaranthus* spp . genotypes to *Meloidogyne* spp . and verification of resistance in genotype Thohoyandou. *Crop Protection*, *115*(1), 64–74.
- Oldham, M. C., Horvath, S., & Geschwind, D. H. (2006). Conservation and evolution of gene coexpression networks in human and chimpanzee brains. *Proceedings of the National Academy of Sciences of the United States of America*, *103*(47), 17973–17978.
- Oosterbeek, M., Lozano-Torres, J. L., Bakker, J., & Govere, A. (2021). Sedentary Plant-Parasitic Nematodes Alter Auxin Homeostasis via Multiple Strategies. *Frontiers in Plant Science*, *12*(1), 1–15.
- Osman, H. A., Ameen, H. H., Mohamed, M., El-Mohamedy, R., & Elkelany, U. S. (2018). Field control of *Meloidogyne incognita* and root rot disease infecting eggplant using nematicide, fertilizers, and microbial agents. *Egyptian Journal of Biological Pest Control*, *28*(1), 1–6.
- Ozalvo, R., Cabrera, J., Escobar, C., Christensen, S. A., Borrego, E. J., Kolomiets, M. V., Castresana, C., Iberkleid, I., & Horowitz, S. B. (2014). Two closely related members of *Arabidopsis* 13-lipoxygenases (13-LOXs), LOX3 and LOX4, reveal distinct functions in response to plant-parasitic nematode infection. *Molecular Plant Pathology*, *15*(4), 319–332.
- Patzewitz, E. M., Wong, E. H., & Müller, S. (2012). Dissecting the role of glutathione biosynthesis in *Plasmodium falciparum*. *Molecular Microbiology*, *83*(2), 304–318.
- Paul, S., Pflieger, L., Dansithong, W., Figueroa, K. P., Gao, F., Coppola, G., & Pulst,



- S. M. (2016). Co-expression networks in generation of induced pluripotent stem cells. *Biology Open*, 5(3), 300–310.
- Perfus-barbeoch, L., Deleury, E., Magliano, M., Engler, G., Vieira, P., Danchin, E. G. J., Rocha, M. Da, Coquillard, P., & Abad, P. (2012). Rapid report A root-knot nematode-secreted protein is injected into giant cells and targeted to the nuclei. *New Phytologist*, 194(4), 924–931.
- Peterson, H., Kolberg, L., Raudvere, U., Kuzmin, I., & Vilo, J. (2020). gprofiler2 -- an R package for gene list functional enrichment analysis and namespace conversion toolset g: Profiler. *F1000Research*, 9, 1–27.
- Phong, V., Bellafiore, S., Petitot, A., Haidar, R., Bak, A., Abed, A., Gantet, P., Mezzalira, I., Engler, J. D. A., & Fernandez, D. (2014). Meloidogyne incognita - rice ( Oryza sativa ) interaction : a new model system to study plant – root-knot nematode interactions in monocotyledons. *Rice Springer*, 7(23), 1–13.
- Poveda, J., Abril-Urias, P., & Escobar, C. (2020). Biological Control of Plant-Parasitic Nematodes by Filamentous Fungi Inducers of Resistance: Trichoderma, Mycorrhizal and Endophytic Fungi. *Frontiers in Microbiology*, 11(May), 1–14.
- Power, D. M., Cardoso, C. R., & Fe, R. C. (2014). Nematode and Arthropod Genomes Provide New Insights into the Evolution of Class 2 B1 GPCRs. *PLoS ONE*, 9(3), 1–17.
- Preussner, M., Gao, Q., Morrison, E., Herdt, O., Finkernagel, F., Schumann, M., Krause, E., Freund, C., Chen, W., & Heyd, F. (2020). Splicing-accessible coding 3'UTRs control protein stability and interaction networks. *Genome Biology*, 21(1), 1–24.

- Prommana, P., Uthaipibull, C., Wongsombat, C., Kamchonwongpaisan, S., Yuthavong, Y., Knuepfer, E., Holder, A. A., & Shaw, P. J. (2013). Inducible Knockdown of Plasmodium Gene Expression Using the glmS Ribozyme. *PLoS ONE*, 8(8), 1–10.
- Pulavarty, A., Egan, A., Karpinska, A., Horgan, K., & Kakouli-duarte, T. (2021). Host Interaction , Management Approaches and Their Occurrence in Two Sites in the Republic of Ireland. *MDPI Plants*, 10(11), 2352.
- Rashidifard, M., Fourie, H., Daneel, M. S., & Marais, M. (2019). Morphological and morphometrical identification of Meloidogyne populations from various crop production areas in South Africa with emphasis on M. enterolobii. *Zootaxa*, 4658(2), 251–274.
- Rashidifard, M., Marais, M., Daneel, M. S., Mienie1, C. M. S., & Fourie, H. (2019). Molecular characterisation of Meloidogyne enterolobii and other Meloidogyne spp . from South Africa. *Tropical Plant Pathology*, 44(1), 214-224.
- Raudvere, U., Kolberg, L., Kuzmin, I., Arak, T., Adler, P., Peterson, H., & Vilo, J. (2019). G:Profiler: A web server for functional enrichment analysis and conversions of gene lists (2019 update). *Nucleic Acids Research*, 47(W1), W191–W198.
- Reimand, J., Arak, T., Adler, P., Kolberg, L., Reisberg, S., Peterson, H., & Vilo, J. (2016). g:Profiler-a web server for functional interpretation of gene lists (2016 update). *Nucleic Acids Research*, 44(W1), W83–W89.
- Reimand, J., Arak, T., & Vilo, J. (2011). G:Profiler - A web server for functional interpretation of gene lists (2011 update). *Nucleic Acids Research*, 39(SUPPL. 2), 307–315.

- Ren, G. X., Guo, X. P., & Sun, Y. C. (2017). Regulatory 3' untranslated regions of bacterial mRNAs. *Frontiers in Microbiology*, 8(1), 1276.
- Rhee, S. Y., & Mutwil, M. (2013). Towards revealing the functions of all genes in plants. *Trends in Plant Science*, 23(3), 1–10.
- Robinson, M. D., McCarthy, D. J., & Smyth, G. K. (2009). edgeR: A Bioconductor package for differential expression analysis of digital gene expression data. *Bioinformatics*, 26(1), 139–140.
- Rodiuc, N., Vieira, P., Banora, M. Y., & de Almeida Engler, J. (2014). On the track of transfer cell formation by specialized plant-parasitic nematodes. *Frontiers in Plant Science*, 5(1), 1–14.
- Russo, P. S. T., Ferreira, G. R., Cardozo, L. E., Bürger, M. C., Arias-carrasco, R., Maruyama, S. R., Hirata, T. D. C., Lima, D. S., Passos, F. M., Fukutani, K. F., Lever, M., Silva, J. S., Maracaja-coutinho, V., & Nakaya, H. I. (2018). CEMiTool : a Bioconductor package for performing comprehensive modular co-expression analyses. *BMC Bioinformatics*, 19(56), 1–13.
- Rutter, W. B., Hewezi, T., Abubucker, S., Maier, T. R., Huang, G., Mitreva, M., Hussey, R. S., & Baum, T. J. (2015). Mining novel effector proteins from the esophageal gland cells of *Meloidogyne incognita*. 27(9), 965–974.
- Sánchez-Moreno, S., Jiménez, L., Alonso-Prados, J. L., & García-Baudín, J. M. (2010). Nematodes as indicators of fumigant effects on soil food webs in strawberry crops in Southern Spain. *Ecological Indicators*, 10(2), 148–156.
- Santos, M. F. A. do., Mattos, V. da S., Monteiro, J. M. S., Almeida, M. R. A., Jorge, A. S., Cares, J. E., Sereno, P. C., Coyne, D., & Carneiro, R. M. D. G. (2019). Diversity

- of *Meloidogyne* spp. from peri-urban areas of sub-Saharan Africa and their genetic similarity with populations from the Latin America. *Physiological and Molecular Plant Pathology*, *105*, 110–118.
- Sarde, S. J., Kumar, A., Remme, R. N., & Dicke, M. (2018). Genome-wide identification , classification and expression of lipoxygenase gene family in pepper. *Plant Molecular Biology*, *98*(4), 375–387.
- Sato, K., Kadota, Y., & Shirasu, K. (2019). Plant Immune Responses to Parasitic Nematodes. *Frontiers in Plant Science*, *10*(1), 1–14.
- Sengupta, P., Chou, J. H., & Bargmann, C. I. (1996). odr-10 Encodes a seven transmembrane domain olfactory receptor required for responses to the odorant diacetyl. *Cell*, *84*(6), 899–909.
- Seo, Y., & Kim, Y. H. (2014). Control of *Meloidogyne incognita* using mixtures of organic acids. *Plant Pathology Journal*, *30*(4), 450–455.
- Sereno, P. C., Mulet, K., Danchin, E. G. J., Koutsovoulos, G. D., Karaulic, M., Da, M., Bailly, M., Loris, B., Laetitia, P., Barbeoch, P., & Abad, P. (2019). Gene copy number variations as signatures of adaptive evolution in the parthenogenetic , plant - parasitic nematode *Meloidogyne incognita*. *Molecular ecology*, *28*(10), 2559–2572.
- Serin, E. A. R., Nijveen, H., Hilhorst, H. W. M., & Ligterink, W. (2016). Learning from Co-expression Networks : Possibilities and Challenges. *Frontiers in Plant Science*, *7*(1), 1–18.
- Seyfried, N. T., Dammer, E. B., Swarup, V., Nandakumar, D., Duong, D. M., Yin, L., Deng, Q., Nguyen, T., Hales, C. M., Wingo, T., Glass, J., Gearing, M.,

- Thambisetty, M., Troncoso, J. C., Geschwind, D. H., Lah, J. J., & Levey, A. I. (2017). A Multi-network Approach Identifies Protein-Specific Co-expression in Asymptomatic and Symptomatic Alzheimer's Disease. *Cell Systems*, 4(1), 60-72.e4.
- Shah, S. J., Anjam, M. S., Mendy, B., Anwer, M. A., Habash, S. S., Lozano-torres, J. L., Grundler, F. M. W., & Siddique, S. (2017). Damage-associated responses of the host contribute to defence against cyst nematodes but not root-knot nematodes. *Journal of Experimental Botany*, 68(21), 5949–5960.
- Shannon, P., Markiel, A., Ozier, O., Baliga, N. S., Wang, J. T., Daniel, R., Nada, A., Schwikowski, B., & Trey, I. (2003). Cytoscape: A Software Environment for Integrated Models. *Genome Research*, 13(22), 426.
- Siddique, S., & Grundler, F. M. W. (2018). ScienceDirect Parasitic nematodes manipulate plant development to establish feeding sites. *Current Opinion in Microbiology*, 46, 102–108.
- Smedley, D., Haider, S., Durinck, S., Pandini, L., Provero, P., Allen, J., Arnaiz, O., Awedh, M. H., Baldock, R., Barbiera, G., Bardou, P., Beck, T., Blake, A., Bonierbale, M., Brookes, A. J., Bucci, G., Buetti, I., Burge, S., Cabau, C., ... Kasprzyk, A. (2015). The BioMart community portal: An innovative alternative to large, centralized data repositories. *Nucleic Acids Research*, 43(W1), W589–W598.
- Smyth, G. K., Ritchie, M. E., Law, C. W., Alhamdoosh, M., Su, S., Dong, X., & Tian, L. (2018). RNA-seq analysis is easy as 1-2-3 with limma, Glimma and edgeR. *F1000Research*, 5, 1–30.

- Srinivasan, S. (2015). Regulation of Body Fat in *Caenorhabditis elegans*. *Annual Review Physiology*, 77(1), 161–178.
- Srinivasan, S. (2020). Neuroendocrine control of lipid metabolism: lessons from *Caenorhabditis elegans*. *Journal of Neurogenetics*, 34(3–4), 482–488.
- Sutherland, B. J. G., Prokkola, J. M., Audet, C., & Bernatchez, L. (2019). Sex-specific co-expression networks and sex-biased gene expression in the salmonid Brook Charr *Salvelinus fontinalis*. *G3: Genes, Genomes, Genetics*, 9(3), 955–968.
- Szitenberg, A., Salazar-Jaramillo, L., Blok, V. C., Laetsch, D. R., Joseph, S., Williamson, V. M., Blaxter, M. L., & Lunt, D. H. (2017). Comparative genomics of apomictic root-knot nematodes: Hybridization, ploidy, and dynamic genome change. *Genome Biology and Evolution*, 9(10), 2844–2861.
- Tan, N., Chung, M. K., Smith, J. D., Hsu, J., Serre, D., Newton, D. W., Castel, L., Soltesz, E., Pettersson, G., Gillinov, A. M., Van Wagoner, D. R., & Barnard, J. (2013). Weighted gene coexpression network analysis of human left atrial tissue identifies gene modules associated with atrial fibrillation. *Circulation: Cardiovascular Genetics*, 6(4), 362–371.
- Teillet, A., Dybal, K., Kerry, B. R., Miller, A. J., Curtis, R. H. C., & Hedden, P. (2013). Transcriptional Changes of the Root-Knot Nematode *Meloidogyne incognita* in Response to *Arabidopsis thaliana* Root Signals. *PLoS ONE*, 8(4), 1–11.
- Teixeira, M. A., Wei, L., & Kaloshian, I. (2016). Root-knot nematodes induce pattern-triggered immunity in *Arabidopsis thaliana* roots. *New*, 211(1), 276–287.
- Tian, T., Liu, Y., Yan, H., You, Q., Yi, X., Du, Z., Xu, W., & Su, Z. (2017). AgriGO v2.0: A GO analysis toolkit for the agricultural community, 2017 update. *Nucleic*

*Acids Research*, 45(W1), W122–W129.

- Tran, T., Chen, S., & Wang, X. (2016). Root assays to study pattern-triggered immunity in plant-nematode interactions. *Plant Pathology Journal*, 15(9), 1–6.
- Vejnar, C. E., Messih, M. A., Takacs, C. M., Yartseva, V., Oikonomou, P., Christiano, R., Stoeckius, M., Lau, S., Lee, M. T., Beaudoin, J. D., Musaev, D., Darwich-Codore, H., Walther, T. C., Tavazoie, S., Cifuentes, D., & Giraldez, A. J. (2019). Genome wide analysis of 3' UTR sequence elements and proteins regulating mRNA stability during maternal-to-zygotic transition in zebrafish. *Genome Research*, 29(7), 1100–1114.
- Vieira, P., Danchin, E. G. J., Neveu, C., Crozat, C., Jaubert, S., Hussey, R. S., Engler, G., Abad, P., De Almeida-Engler, J., Castagnone-Sereno, P., & Rosso, M. N. (2011). The plant apoplasm is an important recipient compartment for nematode secreted proteins. *Journal of Experimental Botany*, 62(3), 1241–1253.
- Vieira, P., & Gleason, C. (2019). ScienceDirect Plant-parasitic nematode effectors — insights into their diversity and new tools for their identification. *Current Opinion in Plant Biology*, 50, 37–43.
- Vinciguerra, M. T. (1979). Role of nematodes in the biological processes of the soil. *Bolletino Di Zoologia*, 46(4), 363–374.
- Vlaar, L. E., Bertran, A., Rahimi, M., Dong, L., Kammenga, J. E., & Helder, J. (2021). On the role of dauer in the adaptation of nematodes to a parasitic lifestyle. *Parasites & Vectors*, 45(3), 1–20.
- Wagner, J. C., Goldfless, S. J., Ganesan, S. M., Lee, M. C. S., Fidock, D. A., & Niles, J. C. (2013). An integrated strategy for efficient vector construction and multi-

- gene expression in *Plasmodium falciparum*. *Malaria Journal*, 12(1), 1–2.
- Watts, J. L., & Ristow, M. (2017). Lipid and Carbohydrate Metabolism in *Caenorhabditis elegans*. *Genetics Society of America*, 207(1), 413–446.
- Wennerberg, K., Rossman, K. L., & Der, C. J. (2005). The Ras superfamily at a glance. *Journal of Cell Science*, 118(5), 843–846.
- Westphal, A. (2011). Sustainable approaches to the management of plant-parasitic nematodes and disease complexes. *Journal of Nematology*, 43(2), 122–125.
- Wu, F., Ma, C., & Tan, C. (2016). Network motifs modulate druggability of cellular targets. *Scientific Reports*, 6(July), 1–11.
- Wu, Z., Hai, E., Di, Z., Ma, R., Shang, F., Wang, Y., Wang, M., Liang, L., Rong, Y., Pan, J., Wu, W., Su, R., Wang, Z., Wang, R., Zhang, Y., & Li, J. (2020). Using WGCNA (weighted gene co-expression network analysis) to identify the hub genes of skin hair follicle development in fetus stage of Inner Mongolia cashmere goat. *PLoS ONE*, 15(12), 1–19.
- Xia, X. (2017). Bioinformatics and Drug Discovery. *Current Topics in Medicinal Chemistry*, 17(15), 1709–1726.
- Xiong, J., Zhou, Q., Luo, H., Xia, L., Li, L., Sun, M., & Yu, Z. (2015). Systemic nematicidal activity and biocontrol efficacy of *Bacillus firmus* against the root-knot nematode *Meloidogyne incognita*. *World Journal of Microbiology and Biotechnology*, 31(4), 661–667.
- Yergert, K. M., Doll, C. A., O'Rourke, R., Hines, J. H., & Appel, B. (2021). Identification of 3' UTR motifs required for mRNA localization to myelin sheaths



- in vivo. *PLoS Biology*, 19(1), e3001053.
- Yin, K., Zhang, Y., Zhang, S., Bao, Y., Guo, J., Zhang, G., Li, T., & Zheng, L. W. (2019). Using weighted gene co-expression network analysis to identify key modules and hub genes in tongue squamous cell carcinoma. *Medicine*, 98(37), 1–9.
- Zhang, B., & Horvath, S. (2005). A general framework for weighted gene co-expression network analysis. *Statistical Applications in Genetics and Molecular Biology*, 4(1), 1–9.
- Zhang, B., Tian, Y., & Zhang, Z. (2014). Network biology in medicine and beyond. *Circulation: Cardiovascular Genetics*, 7(4), 536–547.
- Zhang, X. D., Song, J., Bork, P., & Zhao, X. M. (2016). The exploration of network motifs as potential drug targets from post-translational regulatory networks. *Scientific Reports*, 6(1), 1–12.
- Zhang, Y., Wang, Y., Xie, F., Li, C., Zhang, B., Nichols, R. L., & Pan, X. (2016). Identification and characterization of microRNAs in the plant parasitic root-knot nematode *Meloidogyne incognita* using deep sequencing. *Functional and Integrative Genomics*, 16(2), 127–142.
- Zhao, L., Zhang, X., Wei, Y., Zhou, J., Zhang, W., Qin, P., Chinta, S., Kong, X., Liu, Y., Yu, H., Hu, S., Zou, Z., Butcher, R. A., & Sun, J. (2016). Ascarosides coordinate the dispersal of a plant-parasitic nematode with the metamorphosis of its vector beetle. *Nature Communications*, 7(12341), 1–8.
- Zhao, W., Li, Z., Fan, J., Hu, C., Yang, R., Qi, X., Chen, H., & Zhao, F. (2015). *Identification of jasmonic acid-associated microRNAs and characterization of the*

*regulatory roles of the miR319/TCP4 module under root-knot nematode stress in tomato. 66(15), 4653–4667.*

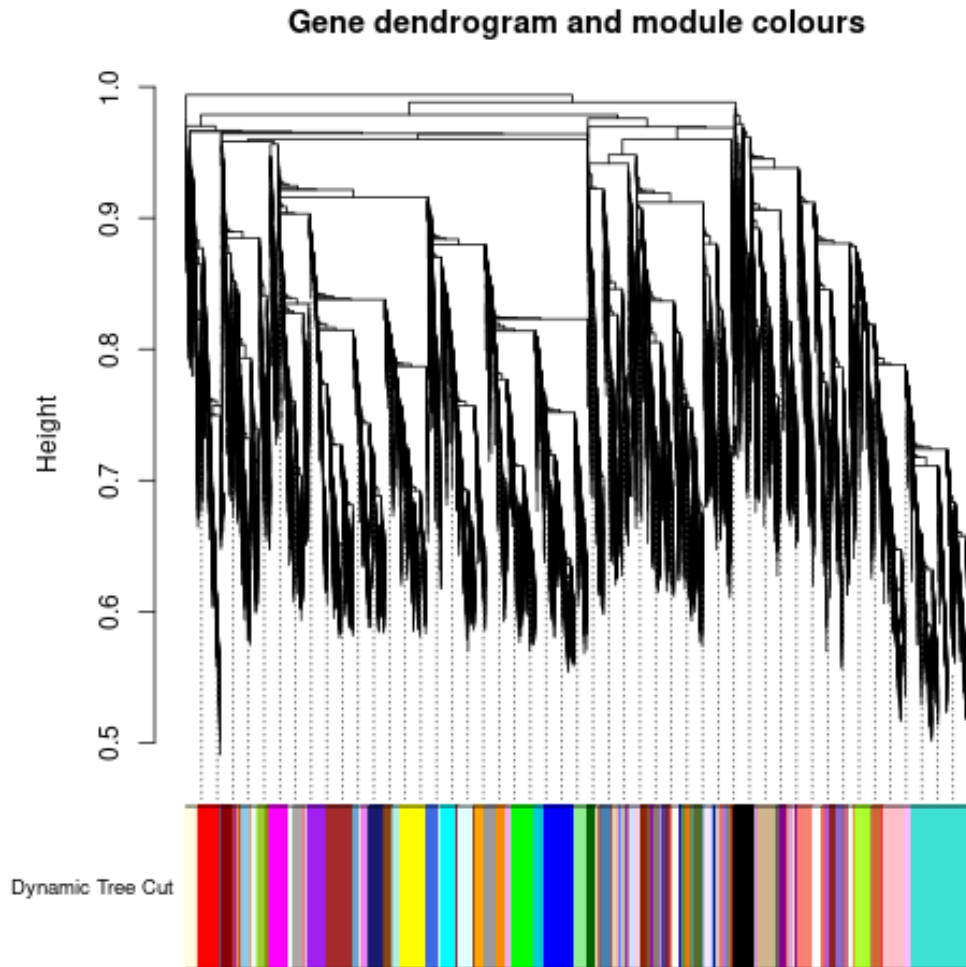
Zhou, Y., Zhou, B., Pache, L., Chang, M., Khodabakhshi, A. H., Tanaseichuk, O., Benner, C., & Chanda, S. K. (2019). Metascape provides a biologist-oriented resource for the analysis of systems-level datasets. *Nature Communications, 10(1).*

Zhu, N., Gao, J., Liang, D., Zhu, Y., Li, B., & Jin, H. (2021). Bioresource Technology Thermal pretreatment enhances the degradation and humification of lignocellulose by stimulating thermophilic bacteria during dairy manure composting. *Bioresource Technology, 319(1), 1–9.*

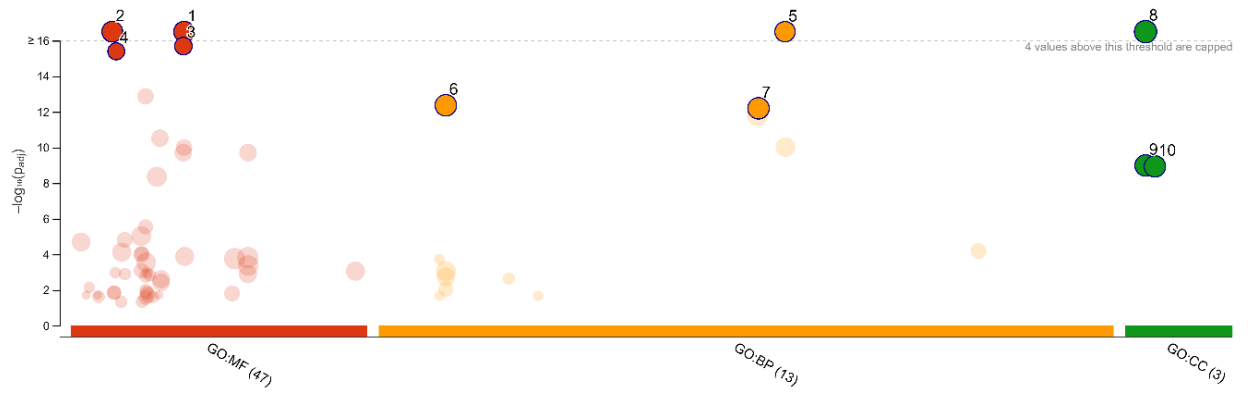
## Appendices

**Appendix A:** Summary of 15 samples from five developmental stages of *Meloidogyne incognita* used in constructing a gene co-expression network, identify gene clusters, and discovery of regulatory motifs

<b>SampleID</b>	<b>Developmental Stage</b>	<b>Nematode Age (Weeks)</b>
SRR5684403	Egg	0 days
SRR5684404	Third juvenile (J3)	3-4
SRR5684405	Fourth juvenile (J4)	5
SRR5684406	Fourth juvenile (J4)	5
SRR5684407	Egg	0 days
SRR5684408	Fourth juvenile (J4)	5
SRR5684409	Adult-female	6-7
SRR5684410	Adult-female	6-7
SRR5684411	Adult-female	6-7
SRR5684412	Second juvenile (J2)	1
SRR5684413	Third juvenile (J3)	3-4
SRR5684414	Second juvenile (J2)	1
SRR5684415	Third juvenile (J3)	3-4
SRR5684416	Second juvenile (J2)	1
SRR5684417	Egg	0



**Appendix B:** An illustration of a hierarchical clustered dendrogram using the Dynamic Tree Cut algorithm applied to the gene-gene co-expression network of *M. incognita*. One hundred and ten (110) modules are represented by the colour panel (Dynamic Tree Cut) in the x axis.

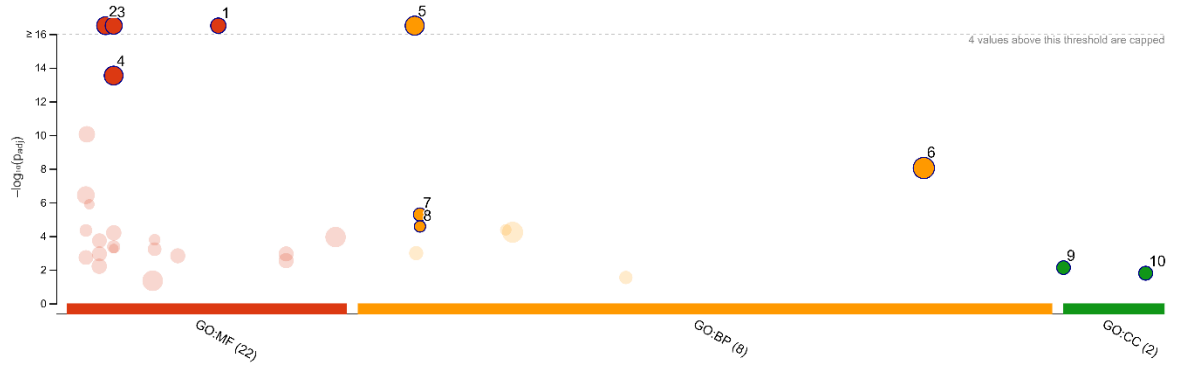


ID	Source	Term ID	Term Name	Padj (query_1)
1	GO:MF	GO:0022857	transmembrane transporter activity	$9.875 \times 10^{-25}$
2	GO:MF	GO:0005215	transporter activity	$6.863 \times 10^{-24}$
3	GO:MF	GO:0022804	active transmembrane transporter activity	$2.033 \times 10^{-16}$
4	GO:MF	GO:0005506	iron ion binding	$4.019 \times 10^{-16}$
5	GO:BP	GO:0055085	transmembrane transport	$4.149 \times 10^{-22}$
6	GO:BP	GO:0006810	transport	$4.317 \times 10^{-13}$
7	GO:BP	GO:0051234	establishment of localization	$6.363 \times 10^{-13}$
8	GO:CC	GO:0016020	membrane	$2.097 \times 10^{-19}$
9	GO:CC	GO:0016021	integral component of membrane	$1.026 \times 10^{-9}$
10	GO:CC	GO:0031224	intrinsic component of membrane	$1.161 \times 10^{-9}$

**Appendix C:** A plot showing highly significant gene ontology terms in the darkslateblue module of the gene co-expression network of *M. incognita*.

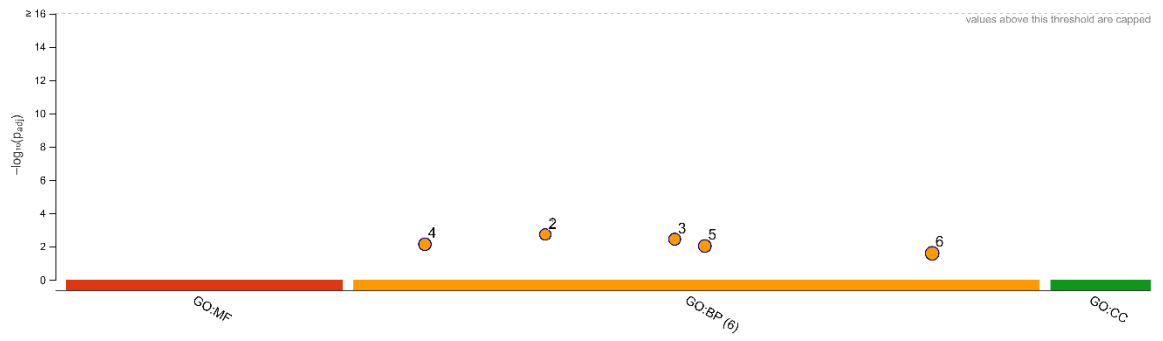


**Appendix D:** A plot showing highly significant gene ontology terms in the darkviolet module of the gene co-expression network of *M. incognita*.



ID	Source	Term ID	Term Name	Padj (query_1)
1	GO:MF	GO:0042302	structural constituent of cuticle	$1.170 \times 10^{-114}$
2	GO:MF	GO:0005198	structural molecule activity	$3.184 \times 10^{-12}$
3	GO:MF	GO:0008237	metallopeptidase activity	$1.668 \times 10^{-20}$
4	GO:MF	GO:0008233	peptidase activity	$2.914 \times 10^{-14}$
5	GO:BP	GO:0006508	proteolysis	$6.426 \times 10^{-17}$
6	GO:BP	GO:1901564	organonitrogen compound metabolic process	$9.054 \times 10^{-9}$
7	GO:BP	GO:0006749	glutathione metabolic process	$5.224 \times 10^{-6}$
8	GO:BP	GO:0006750	glutathione biosynthetic process	$2.679 \times 10^{-5}$
9	GO:CC	GO:0000139	Golgi membrane	$7.506 \times 10^{-3}$
10	GO:CC	GO:0098791	Golgi apparatus subcompartment	$1.617 \times 10^{-2}$

**Appendix E:** A plot showing highly significant gene ontology terms in the mediumorchard module of the gene co-expression network of *M. incognita*.



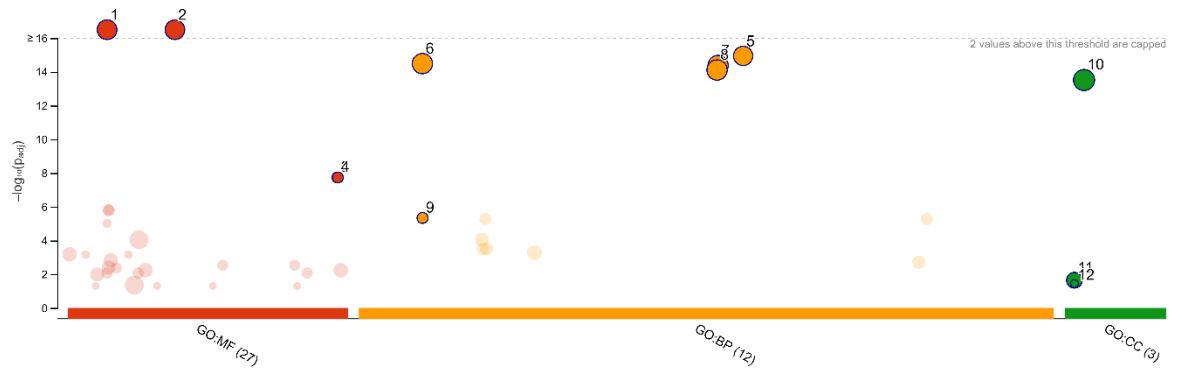
ID	Source	Term ID	Term Name	p <sub>adj</sub> (query_1)
1	GO:BP	GO:0032011	ARF protein signal transduction	$1.893 \times 10^{-3}$
2	GO:BP	GO:0032012	regulation of ARF protein signal transduction	$1.893 \times 10^{-3}$
3	GO:BP	GO:0046578	regulation of Ras protein signal transduction	$3.640 \times 10^{-3}$
4	GO:BP	GO:0007265	Ras protein signal transduction	$7.318 \times 10^{-3}$
5	GO:BP	GO:0051056	regulation of small GTPase mediated signal transd...	$9.358 \times 10^{-3}$
6	GO:BP	GO:1902531	regulation of intracellular signal transduction	$2.590 \times 10^{-2}$

**Appendix F:** A plot showing highly significant gene ontology terms in the medumpurple1 module of the gene co-expression network of *M. incognita*.



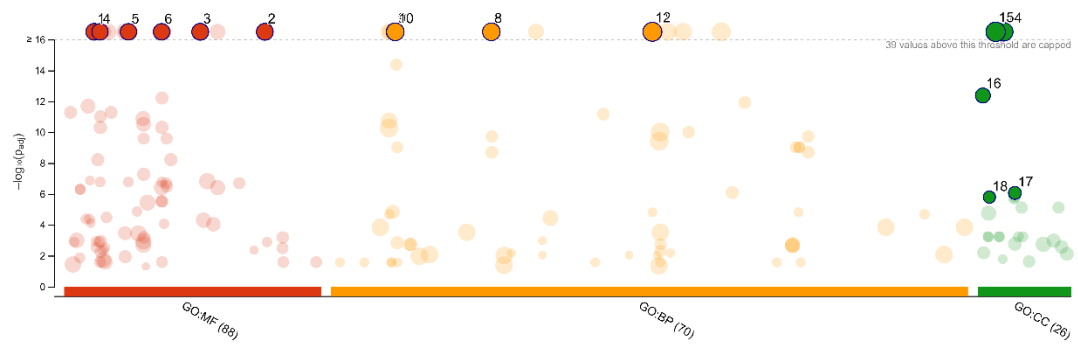


**Appendix G:** A plot showing highly significant gene ontology terms in the navajowhite module of the gene co-expression network of *M. incognita*.



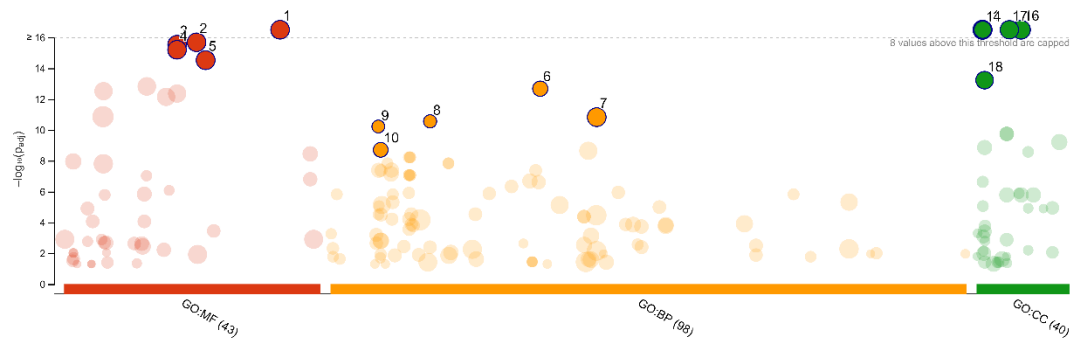
ID	Source	Term ID	Term Name	P <sub>adj</sub> (query_1)
1	GO:MF	GO:0005215	transporter activity	$2.079 \times 10^{-24}$
2	GO:MF	GO:0022857	transmembrane transporter activity	$1.679 \times 10^{-20}$
3	GO:MF	GO:0140303	intramembrane lipid transporter activity	$1.826 \times 10^{-8}$
4	GO:MF	GO:0140326	ATPase-coupled intramembrane lipid transporter a...	$1.826 \times 10^{-8}$
5	GO:BP	GO:0055085	transmembrane transport	$1.129 \times 10^{-15}$
6	GO:BP	GO:0006810	transport	$3.229 \times 10^{-15}$
7	GO:BP	GO:0051234	establishment of localization	$4.201 \times 10^{-15}$
8	GO:BP	GO:0051179	localization	$7.714 \times 10^{-15}$
9	GO:BP	GO:0006817	phosphate ion transport	$4.606 \times 10^{-6}$
10	GO:CC	GO:0016020	membrane	$3.038 \times 10^{-14}$
11	GO:CC	GO:0005783	endoplasmic reticulum	$2.282 \times 10^{-2}$
12	GO:CC	GO:0005785	signal recognition particle receptor complex	$3.656 \times 10^{-2}$

**Appendix H:** A plot showing highly significant gene ontology terms in the plum module of the gene co-expression network of *M. incognita*.



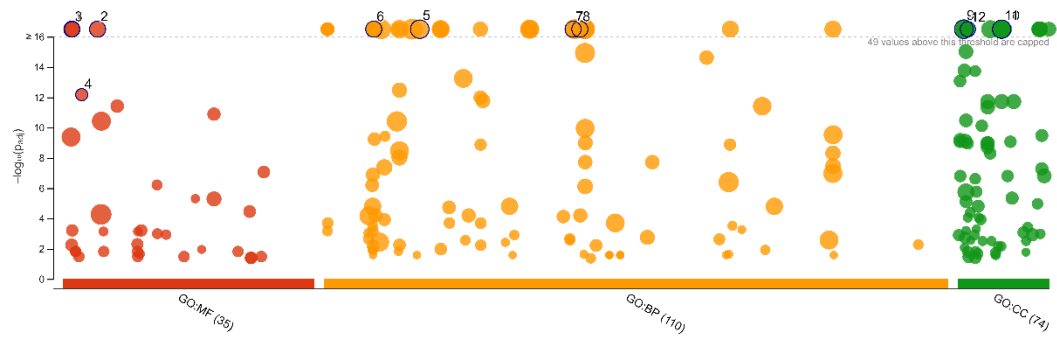
ID	Source	Term ID	Term Name	$p_{adj}$ (query_1)
1	GO:MF	GO:0004888	transmembrane signaling receptor activity	$2.481 \times 10^{-104}$
2	GO:MF	GO:0060089	molecular transducer activity	$1.179 \times 10^{-103}$
3	GO:MF	GO:0038023	signaling receptor activity	$1.179 \times 10^{-103}$
4	GO:MF	GO:0005216	ion channel activity	$3.568 \times 10^{-84}$
5	GO:MF	GO:0015267	channel activity	$1.982 \times 10^{-83}$
6	GO:MF	GO:0022803	passive transmembrane transporter activity	$1.982 \times 10^{-83}$
7	GO:BP	GO:0007186	G protein-coupled receptor signaling pathway	$5.536 \times 10^{-86}$
8	GO:BP	GO:0023052	signaling	$1.174 \times 10^{-80}$
9	GO:BP	GO:0007154	cell communication	$4.490 \times 10^{-80}$
10	GO:BP	GO:0007165	signal transduction	$6.945 \times 10^{-73}$
11	GO:BP	GO:0050794	regulation of cellular process	$1.098 \times 10^{-62}$
12	GO:BP	GO:0050789	regulation of biological process	$1.037 \times 10^{-60}$
13	GO:CC	GO:0016021	integral component of membrane	$2.359 \times 10^{-24}$
14	GO:CC	GO:0031224	intrinsic component of membrane	$3.677 \times 10^{-34}$
15	GO:CC	GO:0016020	membrane	$1.469 \times 10^{-31}$
16	GO:CC	GO:0005576	extracellular region	$4.238 \times 10^{-13}$
17	GO:CC	GO:0034703	cation channel complex	$8.667 \times 10^{-7}$
18	GO:CC	GO:0005929	cilium	$1.608 \times 10^{-6}$

**Appendix I:** A plot showing highly significant gene ontology terms in the blue module of the gene co-expression network of *M. incognita*.



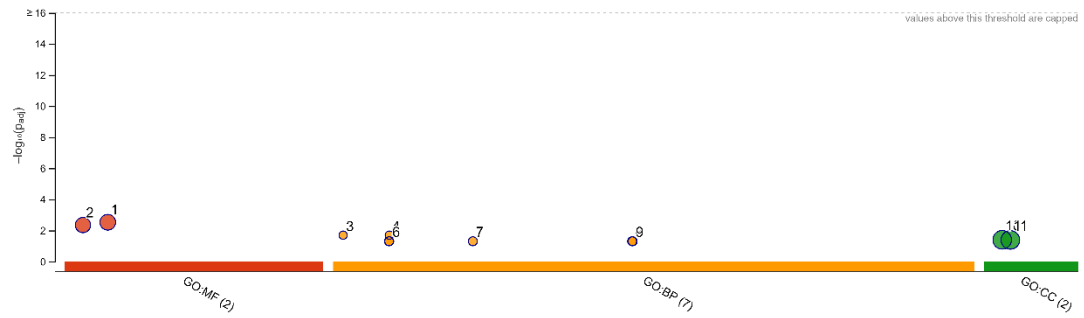
ID	Source	Term ID	Term Name	$p_{adj}$ (query 1)
1	GO:MF	GO:0097367	carbohydrate derivative binding	$8.338 \times 10^{-20}$
2	GO:MF	GO:0035639	purine ribonucleoside triphosphate binding	$2.052 \times 10^{-16}$
3	GO:MF	GO:0032555	purine ribonucleotide binding	$2.944 \times 10^{-16}$
4	GO:MF	GO:0032553	ribonucleotide binding	$6.310 \times 10^{-16}$
5	GO:MF	GO:0043168	anion binding	$2.992 \times 10^{-15}$
6	GO:BP	GO:0034660	ncRNA metabolic process	$2.104 \times 10^{-13}$
7	GO:BP	GO:0044267	cellular protein metabolic process	$1.485 \times 10^{-11}$
8	GO:BP	GO:0010608	posttranscriptional regulation of gene expression	$2.768 \times 10^{-11}$
9	GO:BP	GO:0006261	DNA-dependent DNA replication	$5.994 \times 10^{-11}$
10	GO:BP	GO:0006399	tRNA metabolic process	$1.949 \times 10^{-9}$
11	GO:CC	GO:0005622	intracellular anatomical structure	$7.568 \times 10^{-11}$
12	GO:CC	GO:0043231	intracellular membrane-bounded organelle	$8.490 \times 10^{-36}$
13	GO:CC	GO:0043227	membrane-bounded organelle	$3.593 \times 10^{-33}$
14	GO:CC	GO:0005634	nucleus	$2.575 \times 10^{-24}$
15	GO:CC	GO:0043229	intracellular organelle	$8.131 \times 10^{-24}$
16	GO:CC	GO:0043226	organelle	$9.702 \times 10^{-22}$
17	GO:CC	GO:0032991	protein-containing complex	$1.578 \times 10^{-18}$
18	GO:CC	GO:0005737	cytoplasm	$5.899 \times 10^{-14}$

**Appendix J:** A plot showing highly significant gene ontology terms in the brown module of the gene co-expression network of *M. incognita*.



ID	Source	Term ID	Term Name	Padj (query_1)
1	GO:MF	GO:0003735	structural constituent of ribosome	$1.163 \times 10^{-105}$
2	GO:MF	GO:0005198	structural molecule activity	$1.841 \times 10^{-64}$
3	GO:MF	GO:0003723	RNA binding	$1.965 \times 10^{-21}$
4	GO:MF	GO:0004298	threonine-type endopeptidase activity	$6.721 \times 10^{-13}$
5	GO:BP	GO:0010467	gene expression	$3.250 \times 10^{-94}$
6	GO:BP	GO:0006412	translation	$1.110 \times 10^{-66}$
7	GO:BP	GO:0043043	peptide biosynthetic process	$2.066 \times 10^{-64}$
8	GO:BP	GO:0043604	amide biosynthetic process	$9.737 \times 10^{-69}$
9	GO:CC	GO:0005622	intracellular anatomical structure	$9.194 \times 10^{-1/2}$
10	GO:CC	GO:0043229	intracellular organelle	$6.321 \times 10^{-128}$
11	GO:CC	GO:0043226	organelle	$3.118 \times 10^{-124}$
12	GO:CC	GO:0005840	ribosome	$3.718 \times 10^{-90}$

**Appendix K:** A plot showing highly significant gene ontology terms in the brown4 module of the gene co-expression network of *M. incognita*.



ID	Source	Term ID	Term Name	Padj (query_1)
1	GO:MF	GO:0008237	metallopeptidase activity	$2.959 \times 10^{-3}$
2	GO:MF	GO:0004222	metalloendopeptidase activity	$4.495 \times 10^{-3}$
3	GO:BP	GO:0001573	ganglioside metabolic process	$1.997 \times 10^{-2}$
4	GO:BP	GO:0006689	ganglioside catabolic process	$1.997 \times 10^{-2}$
5	GO:BP	GO:0006672	ceramide metabolic process	$4.972 \times 10^{-2}$
6	GO:BP	GO:0006687	glycosphingolipid metabolic process	$4.972 \times 10^{-2}$
7	GO:BP	GO:0019377	glycolipid catabolic process	$4.972 \times 10^{-2}$
8	GO:BP	GO:0046479	glycosphingolipid catabolic process	$4.972 \times 10^{-2}$
9	GO:BP	GO:0046514	ceramide catabolic process	$4.972 \times 10^{-2}$
10	GO:CC	GO:0016021	integral component of membrane	$3.988 \times 10^{-2}$
11	GO:CC	GO:0031224	intrinsic component of membrane	$4.064 \times 10^{-2}$

**Appendix L:** A plot showing highly significant gene ontology terms in the darkseagreen3 module of the gene co-expression network of *M. incognita*.